

TOPOLOGY OPTIMIZATION OF CONTINUUM STRUCTURES USING
ELEMENT EXCHANGE METHOD

By

Mohammad Rouhi

A Thesis
Submitted to the Faculty of
Mississippi State University
in Partial Fulfillment of the Requirements
for the Degree of Master of Science
in Aerospace Engineering
in the Department of Aerospace Engineering

Mississippi State, Mississippi

May 2009

TOPOLOGY OPTIMIZATION OF CONTINUUM STRUCTURES USING
ELEMENT EXCHANGE METHOD

By

Mohammad Rouhi

Approved:

Masoud Rais-Rohani
Professor of Aerospace Engineering
(Director of Thesis)

Mark F. Horstemeyer
Professor of Mechanical Engineering
(Committee Member)

Thomas E. Lacy
Associate Professor of Aerospace
Engineering
(Committee Member)

Pasquale Cinnella
Professor of Aerospace Engineering
Graduate Coordinator of the Department
of Aerospace Engineering

Sarah A. Rajala
Dean of Bagley College of Engineering

Name: Mohammad Rouhi

Date of Degree: May 2, 2009

Institution: Mississippi State University

Major Field: Aerospace Engineering

Major Professor: Dr. Masoud Rais-Rohani

Title of Study: TOPOLOGY OPTIMIZATION OF CONTINUUM STRUCTURES
USING ELEMENT EXCHANGE METHOD

Pages in Study: 69

Candidate for Degree of Master of Science

In this research, a new zeroth-order (non-gradient based) topology optimization methodology for compliance minimization was developed. It is called the *Element Exchange Method* (EEM). The principal operation in this method is to convert the less effective solid elements into void elements and the more effective void elements into solid elements while maintaining the overall volume fraction constant. The methodology can be integrated with existing FEA codes to determine the stiffness or other structural characteristics of each candidate design during the optimization process.

This thesis provides details of the EEM algorithm, the element exchange strategy, checkerboard control, and the convergence criteria. The results for several two- and three-dimensional benchmark problems are presented with comparisons to those found using other stochastic and gradient-based approaches. Although EEM is not as efficient as some gradient-based methods, it is found to be significantly more efficient than many other non-gradient methods reported in the literature such as GA and PSO.

DEDICATION

To

my beloved parents

ACKNOWLEDGEMENTS

I wish to express my deepest gratitude to the director of my thesis, Dr. Masoud Rais-Rohani who was abundantly helpful and offered invaluable assistance, support and guidance.

I also appreciate Dr. Thomas E. Lacy and Dr. Mark F. Horstemeyer for their serving on my graduate committee and their valuable comments and suggestions.

The funding provided for this study by the US Department of Energy under Grant No. DE-FC26-06NT42755 is gratefully acknowledged.

TABLE OF CONTENTS

	Page
DEDICATION	ii
ACKNOWLEDGEMENTS	iii
LIST OF TABLES	vi
LIST OF FIGURES	vii
 CHAPTER	
I. INTRODUCTION	1
Topology optimization description	1
Overview of topology optimization methods	5
Gradient-based methods.....	6
Non-gradient-based methods	10
Overview of the proposed methodology	12
General principle of element exchange method.....	13
II. ELEMENT EXCHANGE METHOD.....	16
The main algorithm.....	16
Element exchange strategy	20
Checkerboard control.....	21
Random shuffle.....	24
Passive elements	24
Convergence criteria	25
III. RESULTS AND DISCUSSION	27
Two-dimensional cases.....	27
A. Simply-supported beams.....	27
Model 1: Single force applied on top.....	27
Model 2: Single force applied at the bottom.....	31
Model 3: Model 2 with modified boundary conditions	32
B. Cantilevered beams	33

Model 1: Single tip load at the bottom	33
Model 2: Single tip load at the middle.....	34
Model 3: Model 2 with modified dimensions.....	35
Model 4: Model 1 with a circular hole.....	36
Model 5: Opposing loads at the tip	37
Three-dimensional cases	39
A. Cubic Domain	40
B. Cantilevered Beam	41
C. Clamped-Clamped Beam	42
D. Automobile Control Arm	43
Topology optimization with damaged elements	45
Strain energy analysis of the elements.....	47
Strain energy convergence.....	50
Effect of EEM parameters on the solution.....	51
Limitations of EEM	52
IV. CONCLUSIONS AND FUTURE WORK	54
REFERENCES	56
APPENDIX	
MATLAB7.0 CODE* FOR A CANTILEVERED BEAM WITH A CIRCULAR HOLE (SEE TABLE 3.7)	60

LIST OF TABLES

TABLE	Page
3.1 Optimal topologies using EEM and SIMP.....	30
3.2 EEM compared with level set method.....	31
3.3 EEM compared with level set method and BESO.....	32
3.4 Optimal topologies using SIMP method and EEM.....	33
3.5 EEM compared with enhanced GA.....	35
3.6 EEM compared with PSO.....	36
3.7 Optimal topologies for a cantilever beam with a circular hole.....	37
3.8 Optimal topologies for a doubly loaded cantilever beam.....	38
3.9 Optimum topologies for a doubly loaded cantilever beam.....	39
3.10 Energy variation in a target and the whole domain due to solid-void exchange of an arbitrary element.....	48
3.11 Topologies corresponding to each element exchange.....	50

LIST OF FIGURES

FIGURE	Page
1.1 a) Sizing, b) shape and c) topology optimization ¹ (courtesy of Sigmund)	2
1.2 Discretized model of the structural domain with specified loading and support conditions	3
1.3 Microstructures for two-dimensional continuum topology optimization problems: a) Perforated microstructure with rectangular holes in square unit cells, and b) Layered microstructure constructed from two different isotropic materials ¹³ (courtesy of Eschenauer and Olhoff).....	7
1.4 General scheme of topology optimization using SIMP ¹⁴ (courtesy of Shun Wang).....	8
1.5 Spring system a) before and b) after element exchange operation	14
2.1 Flowchart of the EEM.....	17
2.2 Evolution of the topology in EEM from the beginning (1 st iteration) to the end (144 th iteration)	19
2.3 Illustration of checkerboard pattern ³⁴	21
2.4 a) solid checkerboard, b) void checkerboard, c) topology before checkerboard control, d) after solid checkerboard elimination and e) after void checkerboard elimination.....	23
2.5 Two different topologies with nearly identical strain energy values.....	26
3.1 Optimal topologies of MBB-beam using SIMP method (left) and EEM (right)	28
3.2 SIMP results starting from 4 different random distributions of 0-1 densities	30

3.3	EEM compared with optimum microstructure method ⁴⁰ in three-dimensional problems; a) Design domain and boundary conditions, b) Optimum microstructures and c) EEM	40
3.4	EEM compared with optimum microstructure method ⁴⁰ in three-dimensional problems; a) Design domain and boundary conditions, b) EEM , $V_f = 0.3$, c) EEM , $V_f = 0.15$ and d) optimum microstructure, $V_f = 0.3$ where elements with the densities less than 0.8 are filtered out	42
3.5	EEM compared with optimum microstructure method ⁴⁰ in three-dimensional problems; a) Design domain and boundary conditions, b) EEM , $V_f = 0.3$, c) EEM , $V_f = 0.15$ and d) optimum microstructure, $V_f = 0.3$ where elements with the densities less than 0.5 are filtered out	43
3.6	Topology optimization of a control arm; a) FE model ⁴¹ , b) using EEM and c) using OptiStruct ⁴¹ software.....	44
3.7	Starting point (random distribution of the solid elements) for the control arm problem in EEM.....	45
3.8	a) Optimum topology with no damaged elements ($\mathcal{E}_T = 32.6$), b) optimum arrangement of damaged elements, c) random distribution of damaged elements, d) Optimum topology with an initial random distribution of damaged elements ($\mathcal{E}_T = 42.7$) and e) Optimum topology with an initial random distribution of damaged elements and compensated volume fraction ($\mathcal{E}_T = 35.7$), (in cases (a-d); $V_f = 0.5$, $V_{f_damaged} = 0.2$, $f = 0.2$, in case (e); $V_f = 0.6$)	47
3.9	Energy convergence in EEM; rapid convergence from high energy (left) and slow convergence in low energy (right).....	51

CHAPTER I

INTRODUCTION

Topology optimization description

Topology optimization is aimed at finding the optimum distribution of a specified volume fraction of material in a selected design domain. The optimum distribution is often measured in terms of the overall stiffness of the structure such that the higher the stiffness the more optimal the distribution of the allotted material in the domain. It can also be interpreted as finding the optimum load path between the loading and support points for a fixed amount of mass or volume fraction. Topology optimization can be applied to both continuum and discrete (truss like) structures depending on the application.

It should be noted that in topology optimization, both the shape of the exterior boundary and configuration of interior boundaries (i.e., holes, cutouts) can be optimized all at once. Figure 1.1 shows the difference between sizing, shape and topology optimization problems.¹ The differences between these three structural optimization categories mainly consist of the definition of design variables. In the sizing optimization problem, the layout of the structure is prescribed, whereas in shape optimization problem, the exterior and interior boundaries can be treated as design variables.

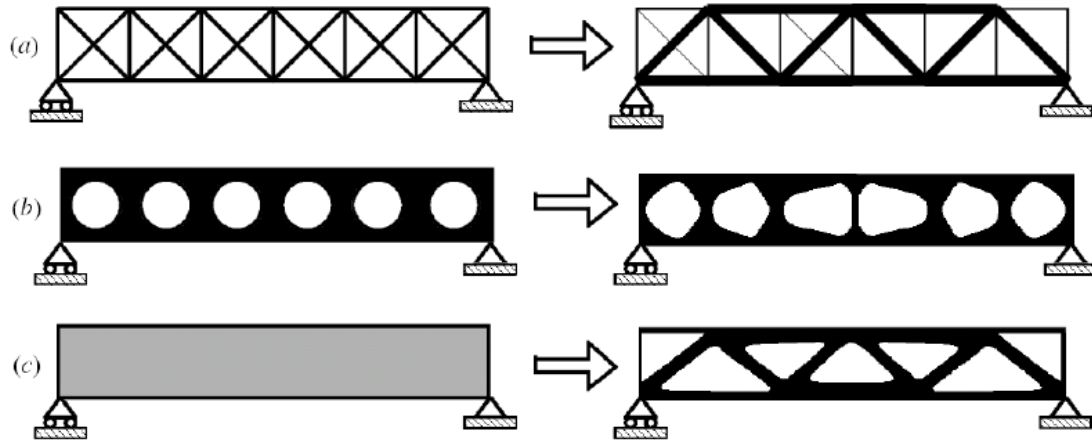


Figure 1.1 a) Sizing, b) shape and c) topology optimization¹ (courtesy of Sigmund)

Introduced by Bendsøe and Kikuchi² and Rozvaney³ topology optimization has gained considerable attention in academia and industry, and is now being applied to the structural and material design⁴, mechanism⁵ and Micro-Electro-Mechanical Systems (MEMS) design.^{6,7} Bendsoe et. al⁸ also reviewed the recent developments of topology optimization techniques for application in some new types of design problems such as design of laminated composite structures, heat transfer problems, design in fluids, acoustics, electromagnetism and photonics.

In the so called “material distribution method”², which is the basis for the design parameterization in topology optimization, the goal is to create regions of uniform material distribution to minimize a specific structural property (e.g., compliance). In this method, a discretized (e.g., finite element) model of the structural domain (Figure 1.2) is used to perform the structural analysis and optimization.

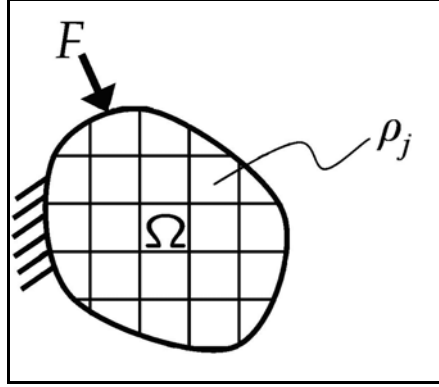


Figure 1.2 Discretized model of the structural domain with specified loading and support conditions

By treating the non-dimensional density of each element as an independent design variable and relating the other physical and engineering properties to element density, a parameterized model is developed that can be used to find such properties as stiffness, thermal conductivity, magnetic permeability, porosity, etc. Theoretically, the non-dimensional density takes a value of one or zero for a solid or void element, respectively. Given an initial distribution of a specified amount of mass, a structural analysis (e.g., finite element analysis (FEA)) is performed to evaluate the response characteristics of the structure. Depending on the topology optimization methodology used, the distribution of solid and void elements is updated and another structural analysis is performed. The sequence of analysis and optimization is continued until the solution converges with the emergence of the optimal topology.

For a continuum structure represented by a domain of finite elements and associated boundary conditions, the topology optimization problem can be expressed mathematically as: Find the optimal distribution of solid and void elements that would

$$\begin{aligned}
\min \quad & f(\boldsymbol{\rho}) = \mathbf{u}^T \mathbf{K} \mathbf{u} = \sum_{j=1}^{N_e} u_j^T K_j u_j = \sum_{j=1}^{N_e} 2\mathcal{E}_j \\
\text{s.t.} \quad & \sum_{j=1}^{N_e} \rho_j V_j \leq V_0 \\
& 0 < \rho_{\min} \leq \rho \leq 1.0
\end{aligned} \tag{1.1}$$

where $f(\boldsymbol{\rho})$ represents the total strain energy, $\boldsymbol{\rho}$ the vector of non-dimensional element densities, which are treated as the design variables, \mathbf{u} the vector of global generalized nodal displacements, \mathbf{K} the global stiffness matrix, with u_j and K_j as the displacement vector and stiffness matrix of the j th element, respectively. With ρ_j and V_j representing the non-dimensional density and volume of the j th element, the constraint in equation 1.1 imposes an upper bound on the acceptable volume fraction in the design domain. The stiffness matrix K_j depends on the density of the j th element in such a way that we may write

$$K_j = \rho_j^p K_e \tag{1.2}$$

where K_e is the stiffness matrix of the j th element if it is fully solid and $p > 1$ is called the penalization power. To avoid having an ill-conditioned stiffness matrix, the void elements are assumed to have a lower bound density, $\rho_{\min} > 0$. Equation 1.2 is the constitutive relation between the density and stiffness in the so-called solid isotropic microstructure (material) with penalization (SIMP) method.³ In this way, the intermediate densities are penalized by power p ; typically, using $p \geq 3$ results in a black-and-white (solid-and-void) topology which is very desirable in structural topology optimization.⁹

As seen in equation 1.1, the number of design variables in the optimization problem is the same as the number of finite elements (FE) in the model. So, one of the most important issues which need to be considered in the implementation of topology

optimization is the choice of optimization algorithm and the number of FEA calculations. This is especially true for topology optimization of three-dimensional structures involving complex boundary conditions.

Overview of topology optimization methods

Topology optimization methods can be divided into two main categories: *gradient based* and *non-gradient based* methods. In gradient-based optimization, the design variables (density ρ in topology optimization) are defined as continuous variables ($0 < \rho_{\min} \leq \rho \leq 1.0$) facilitating the evaluation of the first or possibly second-order derivatives of response functions with respect to design variables and the implementation of mathematical programming techniques for solution of the optimization problem. In non-gradient based approaches, the design variables take discrete values and the methods rely on repeated function evaluations using a stochastic or population-based algorithm. A desired solution for a topology optimization problem is a distribution of either solid ($\rho_j = 1$) or void ($\rho_j = 0$) elements in the FE model of the structure. Mathematically, however, it is difficult to work with integer or discrete design variables. In order to make the functions in the mathematical sense continuous and differentiable, one may need to allow the densities to have intermediate values, which is called *relaxation* of the design variables.¹⁰ A concise overview of these two different approaches is presented next.

Gradient-based methods

Major developments in topology optimization have, for the most part, been directed at the homogenization^{2,11} and the solid isotropic material with penalization (SIMP)^{3,9,12} methods.

Homogenization based optimization (HBO) treats the geometric parameters of a microstructure as design variables and homogenizes the properties in that microstructure. The microstructure as shown in Figure 1.3 is called *hole-in-cell* or *layered* microstructure, which is anisotropic in general.¹³

For the optimization problem, the geometric parameters of the microstructures and their orientation are treated as design variables. The stiffness matrix is numerically calculated based on the homogenization for different sets of the design variables. The structure is iteratively optimized by varying the design variables associated with these microstructures. Since all the design variables are continuous, a gradient-based approach may be utilized to update them in each iteration of the optimization loop.

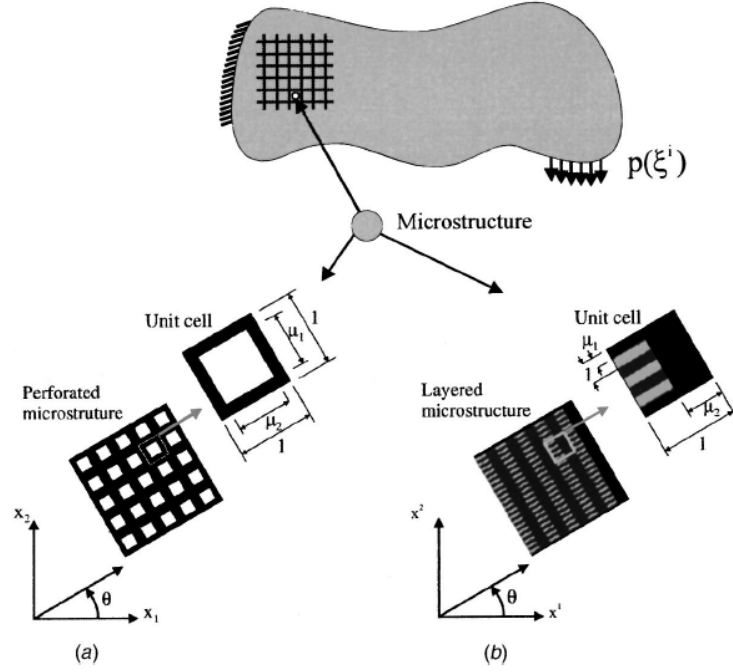


Figure 1.3 Microstructures for two-dimensional continuum topology optimization problems: a) Perforated microstructure with rectangular holes in square unit cells, and b) Layered microstructure constructed from two different isotropic materials¹³ (courtesy of Eschenauer and Olhoff)

Figure 1.4 shows the general scheme of topology optimization using SIMP method.¹⁴ At the first step of the process, the geometry, finite element mesh, and boundary conditions are set up followed by initialization of the density distribution ρ .

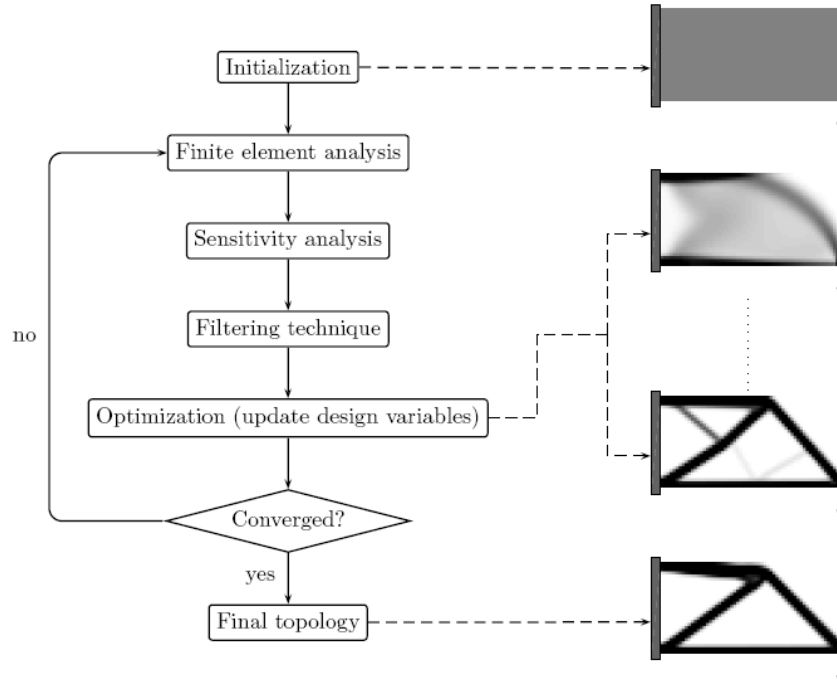


Figure 1.4 General scheme of topology optimization using SIMP¹⁴ (courtesy of Shun Wang)

SIMP usually starts with a uniform distribution of density which is equal to the specified volume fraction. Then the optimization loop begins with assembling and solving the equilibrium equations ($\mathbf{K}u = f$) using FEA. Next, in the sensitivity analysis, the derivatives of the objective function (strain energy) with respect to design variables (ρ_j 's) are computed. Thereafter, an optional filtering technique is applied to remedy the checkerboard problem (discussed in the next chapter). The design variables are then updated in the next step using either the optimality criteria (OC)⁴ or method of moving asymptotes (MMA).¹⁵ The updated design variables and the resulting topology will be analyzed again and the process of analysis and optimization is repeated until convergence is reached.

In general, the optimization process may take many iterations to converge. In terms of computational efficiency, the most expensive part of the optimization is the finite element analysis (FEA) of each candidate design. Depending on the complexity of the structure (i.e., degrees of freedom), the cost of FEA could change. In addition, many topology optimization algorithms have some additional procedures, including the calculation of search direction in the gradient based methods (sensitivity analysis) and/or to filter the undesirable features (e.g. checkerboard regions which will be discussed later) of the final topology. These additional procedures tend to further increase the computational cost of topology optimization.

The SIMP method has become a very popular approach as it is simple to implement, computationally efficient, and easy to integrate with general-purpose FEA codes.¹⁶ However, it suffers from several drawbacks including mesh-dependency of the final topology, undesirable checkerboard patterns requiring the use of filtering techniques, and entrapment in local minima due to its reliance on gradient-based optimization techniques.

Recent improvements to the SIMP method include the use of mesh-independency filtering^{4,17}, higher-order finite elements^{18,19}, perimeter constraint on the density function²⁰, and alternative density-stiffness interpolation schemes.²¹ Commonly used filtering techniques adjust either the sensitivity derivatives of the objective function with respect to the design variables or adjust the design variables themselves in order to eliminate the checkerboard effect. Bruns²² introduced the SINH (pronounced “cinch”) method remedy the drawbacks of both of these filtering approaches while capitalizing on the advantages of each approach. Unlike SIMP, SINH is not an acronym; instead, it

merely references the use of the hyperbolic sine function. Using hyperbolic sine (\sinh) functions, the intermediate density material is made less volumetrically effective than solid or void elements and consequently results in unambiguous and predominantly solid-void designs. By adding a new constraint to the topology optimization problem, labeled the sum of the reciprocal variables (SRV), Fuchs et al.²³ produced sharper 0-1 solutions than the SIMP with greater stiffness for the same amount of material. Efforts to produce better design topologies include relaxation or restriction of the design problem and discretization of the original topology optimization problem combined with heuristic rules to avoid unwanted effects such as checkerboards.¹⁰

Non-gradient-based methods

It has been suggested that the topology optimization problem in equation 1.1 lacks solution in its general continuum form.¹⁰ For a given design, the introduction of more holes without changing the overall material volume fraction will generally improve the objective function. This characteristic is one of the reasons for the solutions to become mesh-dependent. One way to find a solution to this problem is through discretization of the domain and relaxation¹⁰ of the design variables, which was briefly introduced in the previous section. Another way to limit the number of candidate designs (i.e., solutions) is to make design variables binary which means each finite element has either ρ_{\min} or 1 as the value of its density.

The choice of binary design variables facilitates the formation of solid-and-void topologies without any need for a filtering technique. Since the design variables are

binary valued, the objective function—as a consequence—will not be differentiable. Therefore, the gradient methods are not applicable in these cases.

Recent advances in the application of non-gradient approaches to topology optimization problems include the simulated biological growth (SBG)²⁴, particle swarm optimization (PSO)²⁵, evolutionary structural optimization (ESO)²⁶, bidirectional ESO (BESO)²⁷, and metamorphic development (MD)²⁸. Some of these methods together with other algorithms mimicking natural phenomena such as genetic algorithms (GA)²⁹ and cellular automata (CA)³⁰ have been used in sizing and shape optimization problems as well. The use of binary design variables makes it possible for these methods to produce a black-white (solid-void) optimal topology that excludes any gray (i.e., fuzzy or intermediate density) regions without using any filtering technique. In his recent paper, Rozvany¹⁶ gives an in-depth overview of the SIMP method and elaborates on several shortcomings of ESO.^{26,27}

Although non-gradient based approaches are used in conjunction with binary or discrete design variables, there is no restriction to the use of continuous design variables in these methods.²⁵

When the optimum region is flat or contains multiple local (or global) optima, it is possible to find dissimilar optimum configurations.³¹ Werner³² used the full factorial design technique to obtain the global optimum solutions for some benchmark topology optimization problems with very limited number of elements because of large number of function calls (FEA) for full factorial design. Mei et al.³³ developed a binary discrete method for topology optimization by introducing a new sensitivity analysis formula based on the perturbation analysis of the elastic equilibrium increment equation. They

found different optimal topologies for the same problem, demonstrating the non-uniqueness of the binary solution for topology optimization problems.

Overview of the proposed methodology

In this thesis, a new non-gradient based approach called the Element Exchange Method (EEM) is presented. Named after the principal operation in the topology optimization strategy, EEM solution procedure can be integrated with any existing FEA code.

Generally, there are three numerical problems in topology optimization: *Checkerboards*, *Mesh dependence*, and *Local optimum*. Although a more detailed discussion of these problems and how they may be avoided is presented in the next chapter, a brief description of each is given below.

Checkerboard regions are those with solid and void elements ordered in a checkerboard fashion. It is undesirable to have a checkerboard pattern in a topology solution because it has artificially high stiffness, and also such a configuration would be difficult to manufacture.

Mesh dependence refers to the problem of not finding the same solution when the domain is discretized using different mesh densities. Although all finite-element based solutions have mesh dependency, in some gradient-based methods (i.e., SIMP^{4,17}) the filtering scheme used to eliminate medium density (gray) elements is also mesh dependent.

Finally, entrapment into a *local optimum* is always a concern in design optimization when gradient-based techniques are used. This characteristic is less of a

concern in non-gradient based methods since their search algorithms do not rely on function gradients, and they tend to explore a much larger portion of the design space as opposed to that in the vicinity of the initial design point.

There are different techniques to overcome the above mentioned problems which are described briefly in Ref. [10]. In the next chapter, specific details of the EEM algorithm are provided along with description of the strategies used in EEM to address the aforementioned problems. The results for several two- and three-dimensional benchmark problems of varying complexity are presented and comparisons are made with the solutions found using the SIMP and some other methods as reported in the literature.

General principle of element exchange method

A simple structural system idealized by a combination of four linearly elastic springs is shown in Figure 1.5. The discrete spring system is attached to a rigid wall on the left side and is pulled on the right side by the force F . The total strain energy, \mathcal{E}_T stored in the system is simply the sum of energy stored in individual springs and expressed as

$$\mathcal{E}_T = \sum_{i=1}^4 \mathcal{E}_i = \frac{1}{2} \sum_{i=1}^4 K_i \delta_i^2 \quad (1.3)$$

where \mathcal{E}_i is the energy in the i th spring which can be defined in terms of the corresponding stiffness, K_i and elongation, δ_i .

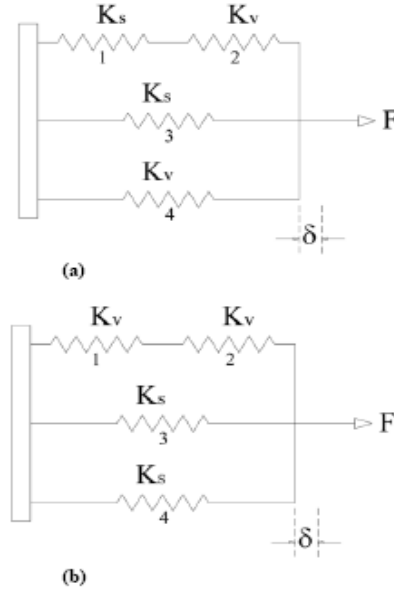


Figure 1.5 Spring system a) before and b) after element exchange operation

Assuming that only two springs can be used for minimizing the strain energy of the system, the problem becomes one of finding which two springs to keep and which ones to eliminate. The two retained springs also create the optimal load path between the loaded and supported points of the system. For simplicity, a stiff “solid” spring is assumed to have a stiffness of K_s while a flexible “void” spring has a stiffness of $K_v = 0.001 K_s$. If the initial distribution is that shown in Figure 1.5(a), then the total strain

energy can be shown to be $\mathcal{E}_T = \frac{K_s}{2} [1 \times 10^{-6} + 1 \times 10^{-3} + 1 \times 10^0 + 1 \times 10^{-3}] \delta^2 \approx \frac{1}{2} K_s \delta^2 = \frac{1}{2} \frac{F^2}{K_s}$.

Since spring 1 is a solid spring with the lowest strain energy between the two solid springs, in the next iteration, it will be converted into a void spring while spring 4 representing a void spring with the highest strain energy between the two void springs will be converted into a solid spring. Figure 1.5(b) shows the updated layout after the element exchange operation is performed. Now, the total strain energy stored in the

system can be shown to be $\mathcal{E}_T = \frac{K_s}{2} [2.5 \times 10^{-4} + 2.5 \times 10^{-4} + 1 \times 10^0 + 1 \times 10^0] \delta^2 \approx K_s \delta^2 = \frac{1}{4} \frac{F^2}{K_s}$.

While the number of “solid” springs is kept constant, the total strain energy of the system is reduced by 50%, signifying greater stiffness and smaller compliance. Hence, by identifying and switching the less influential solid spring into a void spring and the more influential void spring into a solid spring, a better (more efficient) load path is created.

The purpose of this simple example is to illustrate the general principle of element exchange. By extending the loading system to a continuum domain represented by a finite element mesh, it would be possible to use the element exchange as part of a solution procedure for finding the optimal topology.

CHAPTER II

ELEMENT EXCHANGE METHOD

The main algorithm

As stated earlier in equation 1.1, to avoid having an ill-conditioned stiffness matrix, the void elements are assumed to have a lower bound density, $\rho_{\min} > 0$. As in the SIMP method, it is assumed that the stiffness-density relationship holds but with no penalization factor (i.e., $E_j = \rho_j E$, where E is the Young's modulus of the solid material). In EEM, ρ_j is treated as a binary design variable with $\rho_{\min} = 0.001$. Moreover, the inequality constraint is replaced by an equality constraint ($\sum_{j=1}^{N_e} \rho_j V_j = V$) so that in each iteration this equality constraint, which is the volume fraction constraint, is not violated (In the case of non-uniform meshes, the violation will be allowed within a small tolerance by exchanging different number of void versus solid elements). The EEM algorithm for the solution of the topology optimization problem in equation 1.1 is shown in Figure 2.1.

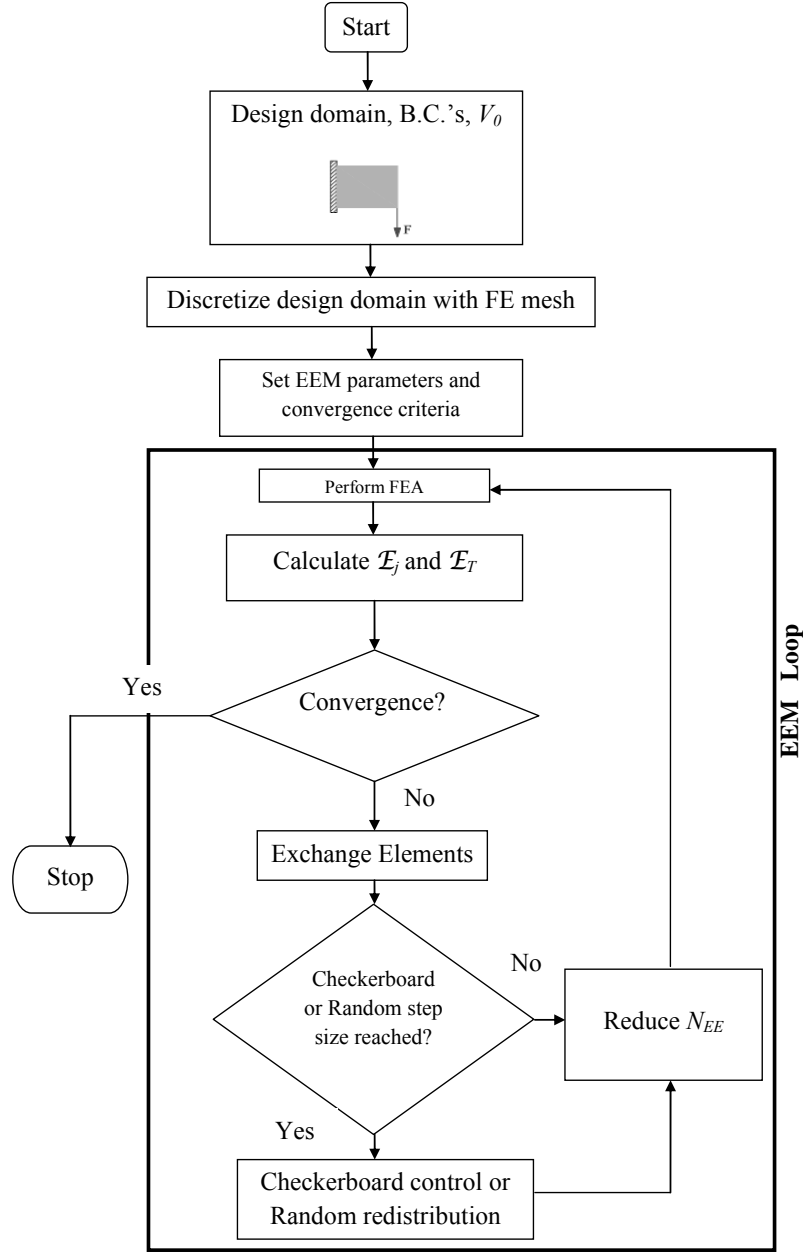


Figure 2.1 Flowchart of the EEM

The algorithm starts with a random distribution of a specified number of solid isotropic elements (with $\rho = 1.0$), consistent with the desired volume fraction V_0 in the design domain. The solution is generally not sensitive to the choice of initial topology and any distribution resulting in $V = V_0$ is acceptable. All void elements are given a non-

dimensional density of 0.001. With the initial topology identified, a static FEA is performed to find the strain energy distribution among the finite elements as well as the total strain energy of the structure as a whole. Based on the selected value for the number of exchange elements, N_{EE} , the algorithm performs a so-called element exchange operation. The N_{EE} solid elements with the lowest strain energy amongst the solid elements are converted into void elements ($\rho_i = \rho_{\min}$) while a volumetrically equivalent number of void elements with the highest strain energy amongst the void elements are converted into solid elements ($\rho_i = 1$) such that the volume fraction remains fixed. Depending upon the domain geometry, it may be possible to set the number of solid-to-void and void-to-solid element conversions equal or different as long as the volume fraction is kept constant. Ordinarily, the revised topology following the element exchange step will have a lower strain energy value, although it is possible to have an opposite trend in some iterations. Strain energy convergence in EEM is described in more detail in the next chapter. The updated topology is analyzed again to find the new values for strain energy distribution and the overall compliance. Once again the solid and void elements with the extreme strain energy amongst each set are exchanged and the procedure continues until the overall compliance value converges to its minimum value. Here, convergence is defined as a nearly stationary topology with changes in the strain energy below the specified threshold. As in the case of the other stochastic methods, a limit is imposed on the number of iterations to stop the program when the selected convergence criterion is too tight. The algorithm is readily applicable to any two- or three-dimensional domain and boundary conditions, irrespective of its geometric or loading complexity.

Figure 2.2 schematically shows the evolution of the topology during optimization process in EEM.

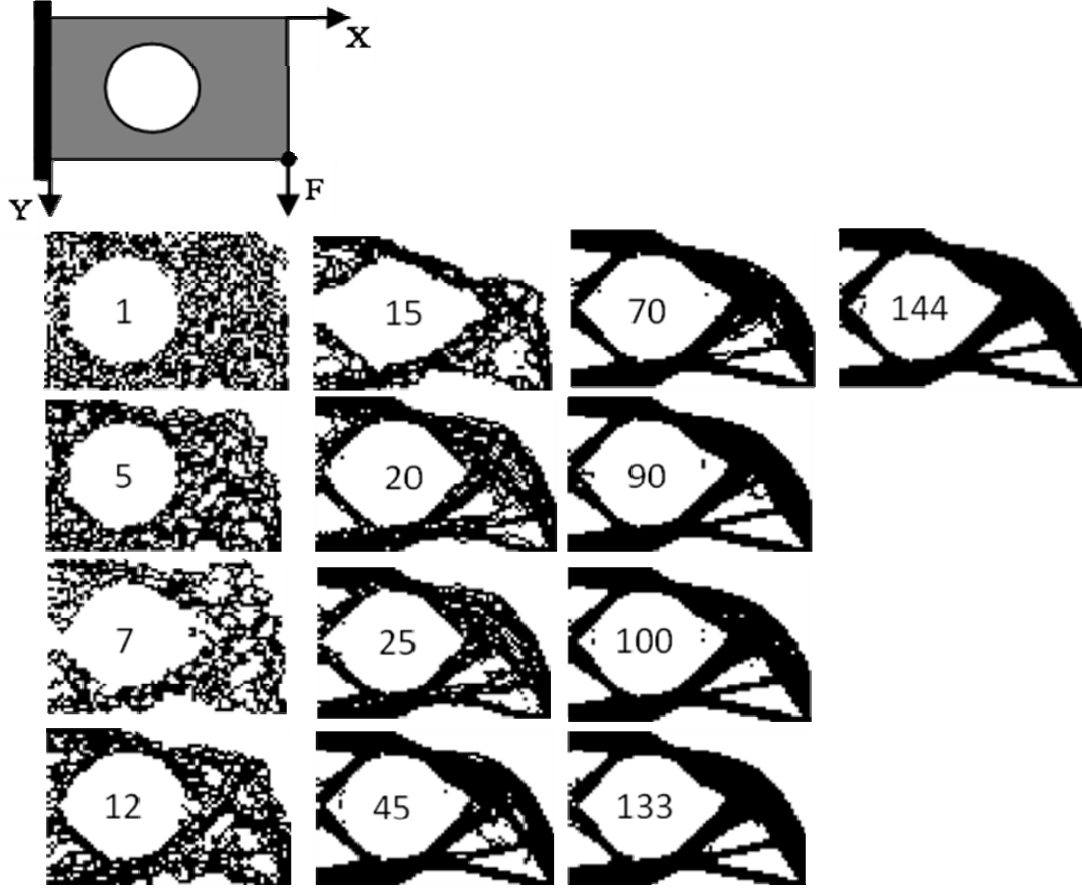


Figure 2.2 Evolution of the topology in EEM from the beginning (1st iteration) to the end (144th iteration)

Although the EEM algorithm pushes the topology towards minimum-compliance, the basic element exchange operation alone may not prevent the development of undesirable checkerboard patterns or the possibility of back and forth oscillation in a subset of elements from solid to void back to solid in repeated iterations. However, with

the help of additional operations—which will be described next—these problems are eliminated.

Element exchange strategy

As stated earlier, in each iteration a number of solid elements will give their position to void elements and vice versa.

If the number of exchanging elements (N_{EE}) is set to a large number, the near-optimum topology will start to form quickly, but it will not converge. This is because at the beginning of the procedure a large number of solid elements will be exchanged with a large number of void elements in such a way that will drastically decrease the strain energy of the structure resulting in a better topology. However, as EEM procedure is continued, the same number of elements (which is large) will be switching places in the remaining iterations. That will lead to an oscillatory behavior in the formation of final topology.

On the other hand, if N_{EE} is set to a small number, the topology will evolve to its optimum state in an extremely slow manner with respect to the mesh size of the problem. It would also be less capable of finding the best optimum solution due to limited number of elements that can be altered in the EEM process.

Therefore, a viable element exchange strategy is to gradually decrease the N_{EE} value when the solution is nearing convergence. In the first iteration ($k = 0$), N_{EE} is set equal to N_{\max} with a gradual reduction toward a specified minimum N_{\min} by following the relationship

$$N_{EE}^k = \text{int} \left[N_{\max} - k \left(\frac{N_{\max} - N_{\min}}{N_s} \right) \right] \quad (2.1)$$

where k and N_s denote the iteration counter and the maximum number of steps required for N_{EE} to gradually decrease from its maximum to minimum value.

Checkerboard control

Depending on the specified volume fraction and the proximity of strain energy levels for different distributions of the same volume of material, it is possible to encounter a checkerboard pattern. In Figure 2.3, the arrows mark the checkerboard regions, which can be verbally described as void/solid elements that do not share their edges with similar elements.

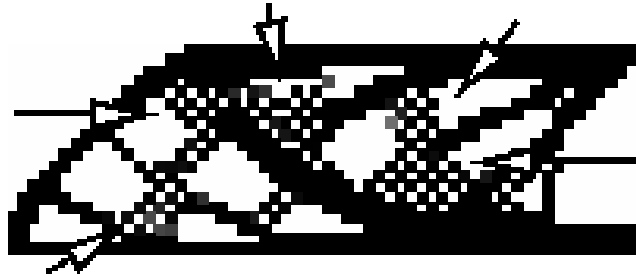


Figure 2.3 Illustration of checkerboard pattern³⁴

Diaz and Sigmund¹⁸ showed that the checkerboard pattern occurs because it has a numerically induced (artificially) high stiffness compared with a material with uniform material distribution. The easiest way to prevent checkerboard is to use higher order elements (8- or 9-node elements for 2-dimensional cases).^{18,19} This, however, increases the computational time drastically.⁹ There are several checkerboard-prevention schemes

that are almost all based on heuristics.⁸ Smoothing the optimal topology (with checkerboard) using image processing techniques is one of these methods and should be avoided since it ignores the underlying problem.^{9,10} Another technique which is one of the most popular methods to remove checkerboard regions is filtering. Sigmund⁹ introduced the checkerboard prevention filter based on filtering techniques from image processing. He modified the design sensitivities used in each iteration of the algorithm for solving the discretized problem.^{9,17} The filter makes design sensitivity of each element dependent on a weighted average of that specific element and its eight neighboring (contacting) quadrilateral elements.

Since EEM is not a gradient-based method, it is not possible to use filtering techniques that rely on design sensitivities. To eliminate the checkerboard problem in EEM, first the solid checkerboard elements are identified and converted into void elements (Figures 2.4 (c,d)), and then the void checkerboard elements are converted into solid elements (Figures 2.4 (d,e)). Then, to maintain the specified volume fraction, the difference between the number of the switched solid and void elements are randomly redistributed in the design domain. It is possible for this random redistribution to result in the creation of small checkerboard regions. However, as EEM procedure is continued, these regions tend to gradually diminish before the final topology emerges.

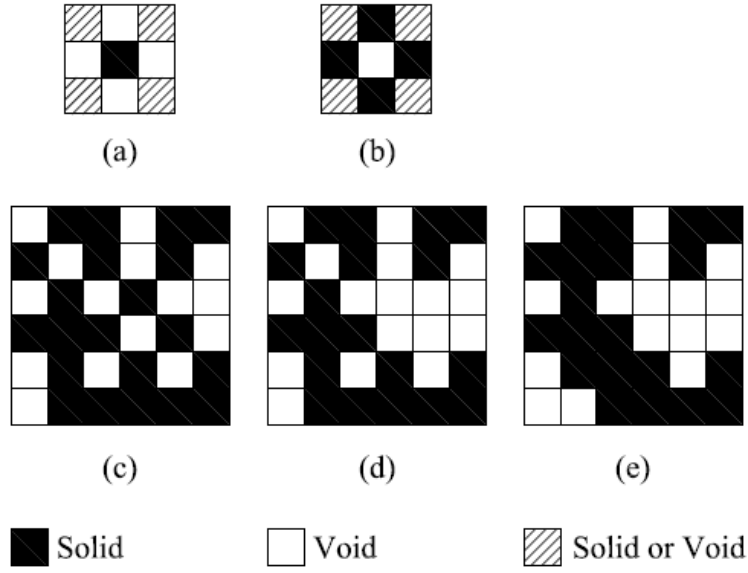


Figure 2.4 a) solid checkerboard, b) void checkerboard, c) topology before checkerboard control, d) after solid checkerboard elimination and e) after void checkerboard elimination

Since in the early iterations the basic topology of the structure has not yet emerged, the checkerboard control is delayed. In other words, in early iterations, the checkerboard regions are not formed because of the FE numerical problems but mostly formed because of random distribution of solid elements. So they are not artificially induced stiff regions but randomly distributed checkerboard elements. Therefore, the checkerboard control function in EEM is called after a set number of iterations, defined by the “checkerboard step size”, L_c , have been completed. This step size is a small fraction of the user specified maximum iterations.

Random shuffle

After a number of iterations have been completed, it is possible for EEM to occasionally encounter a condition where the same sets of solid and void elements switch places in consecutive iterations. To eliminate this problem, a random perturbation or shuffle of a subset of solid and void elements is performed after a specified number of iterations. This action is analogous to the mutation operation in GA or craziness move in PSO.²⁵ Although the random shuffle will not violate the volume fraction constraint, it is likely to cause an abrupt change in the total strain energy due to the redistribution of the solid elements and the potential variation in the structural stiffness.³⁵ It is also likely to lead to the creation of new checkerboard regions, which would need to be eliminated in the subsequent steps. The number of elements to be exchanged randomly, N_R is not constant but varies according to a relationship similar to equation 2.1. Random shuffle also has its own “random step size”, L_R that identifies the points during the iteration process where it is performed.

Passive elements

Some continuum structures may contain both designable and fixed subregions. The latter may be in the form of fixed holes or cutouts and/or fixed solid parts whose geometry and locations, because of some design or manufacturing constraints, cannot be altered during topology optimization. As a matter of convenience and meshing simplicity (or design requirement), the fixed voids (or solids) are represented by a series of passive elements with $\rho_i = \rho_{\min}$ (or $\rho = 1.0$). The passive elements will not be exchanged during the EEM solution process.

Convergence criteria

Increasing the number of iterations in EEM will usually lead to a more refined optimal topology but at the expense of more function calls (i.e., additional FE solutions). Besides imposing a limit on the maximum number of iterations, two additional criteria are also used to establish a two-part convergence condition in EEM-based topology optimization.

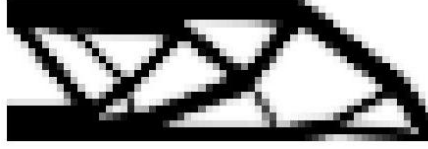
The first criterion considers the relative difference in the element strain energy distributions in two consecutive “elite topologies”. Here, elite topology refers to the topology with the lowest strain energy obtained prior to the current iteration in the EEM procedure. Since it is possible for two distinctly different topologies to have almost equal total strain energies (Figure 2.5), it is necessary to compare the element strain energy distribution, as represented by the vector $\tilde{\mathbf{E}}$, for two consecutive elite topologies as

$$\frac{\|\tilde{\mathbf{E}}_{ce} - \tilde{\mathbf{E}}_{pe}\|}{\|\tilde{\mathbf{E}}_{pe}\|} \leq \epsilon_E \quad (2.2)$$

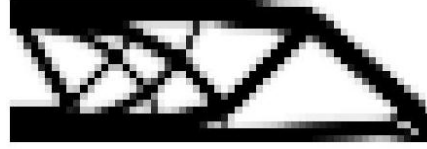
where subscripts “ce” and “pe” refer to the current and previous elite topologies within N_s iterations, respectively.

The second convergence criterion examines the density (design variable) distribution in two consecutive elite topologies. The domain topology is defined by vector $\tilde{\mathbf{D}}$ whose individual terms have binary values depending on the solid (1) or void (0) property of the corresponding elements. Based on this definition, the convergence criterion is defined as

$$\frac{\|\tilde{\mathcal{D}}_{ce} - \tilde{\mathcal{D}}_{pe}\|}{\|\tilde{\mathcal{D}}_{pe}\|} \leq \varepsilon_t \quad (2.3)$$



a) $\mathcal{E} = 196.3$



b) $\mathcal{E} = 196.4$

Figure 2.5 Two different topologies with nearly identical strain energy values

CHAPTER III

RESULTS AND DISCUSSION

Two-dimensional cases

Several benchmark problems are used to evaluate the performance of EEM and to compare the results with those obtained from some other methods. Each two-dimensional design domain is defined according to n_x , n_y , V_0 values representing the number of finite elements in the x and y directions and the limit on volume fraction, respectively. Hereafter, strain energy refers to the non-dimensional strain energy since the nodal displacements and element stiffness are normalized with respect to the element size and the material stiffness. The iteration number (Itr.) for EEM based results coincides with the number of FE analyses performed in the optimization process.

A. Simply-supported beams

Model 1: Single force applied on top

The simply-supported Messerschmitt-Bölkow-Blohm (MBB) beam³⁶ model and loading shown in Figure 3.1 is optimized for minimum compliance. Due to the overall symmetry, the computational model represents one half of the physical domain. For (n_x ,

$n_y, V_0) = (60, 20, 0.5)$, it takes 235 iterations for EEM to produce a 1-0 topology as shown in Figure 3.1 with total strain energy of 191.5.

The SIMP based optimal topology is also shown in Figure 3.1 for comparison. The SIMP results are obtained using the algorithm provided by Sigmund.¹⁷ The filtered optimal topology of SIMP is obtained after 94 iterations with the filtering radius of 1.5, and the strain energy of 203.3. Each iteration in SIMP consists of one FEA, sensitivity analysis, and filtering operation, with FEA being the most computationally expensive part of the iteration.

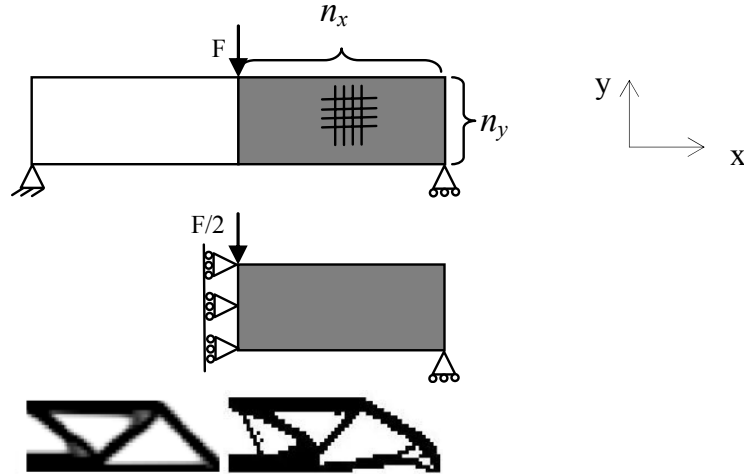


Figure 3.1 Optimal topologies of MBB-beam using SIMP method (left) and EEM (right)

It should be noted that due to the stochastic nature of EEM, the optimal topology and the corresponding number of iterations may vary from one EEM solution to another. However, in each solution, the final topology represents an optimum distribution of material and the resulting value for total strain energy can be used to identify the best possible topology among the solutions obtained. Figure 3.1 may be an evidence for the flatness and noisiness of the solution of the topology optimization problem which has

been discussed in the introduction. The two final topologies are not the same but their strain energies are fairly close.

Additional points to consider in this comparison is that while the filtering technique in SIMP topology is mesh dependent and quite sensitive to the choice of filtering radius r , EEM uses no filtering and its mesh dependency is only tied to the use of FEA.

Also, due to the stochastic nature of EEM, it is possible to find optimum solutions that are different from the SIMP based solutions but with similar or sometimes smaller compliance. It is also worth mentioning that with SIMP, starting with different non-uniform initial designs (randomly distributed solid-void elements with the same volume fractions) may lead to different solutions (local minima). These characteristics are demonstrated by the designs in Figure 3.2 and Table 3.1 using a fine mesh with $(n_x, n_y, V_0) = (90, 30, 0.5)$. While in Table 3.1 all the SIMP solutions are based on an initial design having a uniform density distribution throughout the domain, the EEM solutions are based on random distributions of solid and void elements in the initial design for the specified volume fraction of 50%.

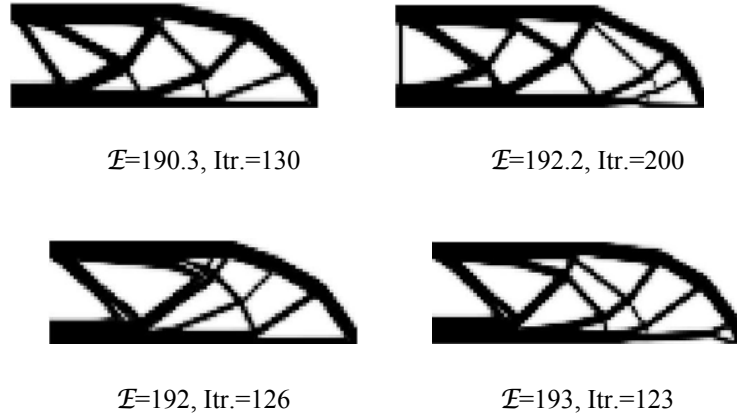








Figure 3.2 SIMP results starting from 4 different random distributions of 0-1 densities

Table 3.1

Optimal topologies using EEM and SIMP

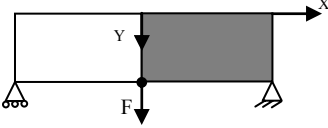


EEM	SIMP
 <p>Itr.=192, $\mathcal{E}_T = 201.3$</p>	 <p>r=1, Itr.=33, $\mathcal{E}_T = 201.3$</p>
 <p>Itr.=227, $\mathcal{E}_T = 191.4$</p>	 <p>r=1.2, Itr.=45, $\mathcal{E}_T = 194.8$</p>
 <p>Itr.=210, $\mathcal{E}_T = 187$</p>	 <p>r=2, Itr.=29, $\mathcal{E}_T = 204.1$</p>

Model 2: Single force applied at the bottom

A simply-supported beam with $(n_x, n_y, V_0) = (50, 50, 0.4)$ is optimized using EEM with the results shown in Table 3.2. The results reported by Wang and Wang³⁷ using the gradient-based level set method with $(n_x, n_y, V_0) = (61, 62, 0.31)$ is also shown in Table 3.2 for comparison. The strain energy of the EEM based solution is 33.4.

Table 3.2

EEM compared with level set method

Design domain & Boundary conditions		
		
<i>Method</i>	<i>EEM</i>	<i>Level Set</i> ³⁷
<i>Itr.</i>	146	200
<i>Topology</i>		

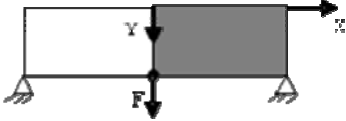


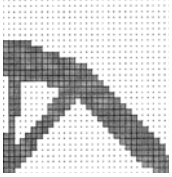
Unfortunately the non-dimensional strain energy in the level set method has not been reported. However, by dividing the final value of the strain energy from their plot of strain energy convergence history by the applied force and assumed elastic modulus, we obtain a non-dimensional strain energy of about 34, which is nearly equal to the value found using EEM.

Model 3: Model 2 with modified boundary conditions

The roller support on the right side of the beam in Model 2 is replaced by a pin support preventing the beam from having any horizontal displacement at the supports. The change in the boundary condition affects the optimum topology as shown in Table 3.3. The result from EEM with $(n_x, n_y, V_0) = (50, 50, 0.4)$ is compared with that reported in the literature by Wang and Wang³⁷ using the level set method with $(n_x, n_y, V_0) = (61, 62, 0.31)$ and by Querin et al.²⁷ using BESO with $(n_x, n_y, V_0) = (31, 32, 0.25)$.

Table 3.3

EEM compared with level set method and BESO

Design domain & Boundary conditions			
			
<i>Method</i>	<i>EEM</i>	<i>Level Set</i> ³⁷	<i>BESO</i> ²⁷
<i>Itr.</i>	104	140	47 ^a
<i>Topology</i>			

^aThe reported “steady state” number. Total number of FE solutions not specified.

Since all the topologies resulted from the three different methods in Table 3.3 are similar, we can conclude that they have the same strain energy. It should be noted that when two topologies are similar, one may simply conclude that their strain energies are the same, but the converse conclusion may not be drawn. In other words, if two

topologies have the same strain energy level, it does not necessarily mean that they look like each other (see Figure 2.5).

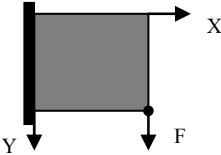




B. Cantilevered beams

Model 1: Single tip load at the bottom

Table 3.4 shows the cantilevered beam and loading condition with EEM results compared with those based on the SIMP method for a volume fraction of 40%. In the case of the SIMP, the results are based on the filtering radius of $r = 1.2$. While the optimal strain energy values are comparable, the total iteration numbers are different. As a result of mesh refinement, the optimal topology changes with minimal change in the final strain energy.

Table 3.4

Optimal topologies using SIMP method and EEM

Design domain & Boundary conditions				
				
(n_x, n_y, V_0)	Coarse mesh (32, 20, 0.4)		Fine mesh (64, 40, 0.4)	
<i>Method</i>	<i>EEM</i>	<i>SIMP</i>	<i>EEM</i>	<i>SIMP</i>
<i>Strain Energy</i>	53.6	57.4	57	55.7
<i>Itr.</i>	178	71	174	57
<i>Topology</i>				

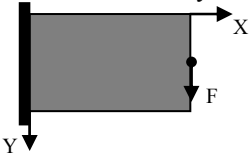
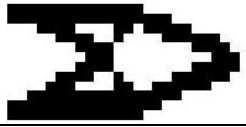
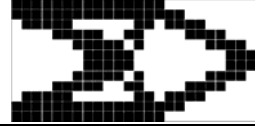
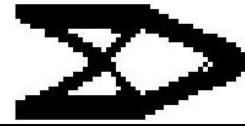
Comparing the results from SIMP, one may observe that although the topologies are not similar to each other, their strain energies are very close to each other. It is a good case to observe the flatness of the solution in a general topology optimization problem. This feature of the problem is more observable when one compares the final topologies of EEM and SIMP with a finer mesh since they look very different but with nearly the same strain energy.

Model 2: Single tip load at the middle

The beam model and corresponding topology optimization results are shown in Table 3.5. Two different mesh densities are considered for EEM resulting in slightly different topologies. The results reported by Wang et al.³⁸ based on the enhanced GA approach are also shown in Table 3.5 for comparison. Although the final geometry and strain energy values are nearly the same, the EEM solution converges much faster. Jakiela et al.³⁹ state that, in general, GA based solutions may require 10 to 100 times the number of function evaluations as would be required by homogenization based solutions. It is notable that the number of function calls (FEA plus any other analysis used in that particular method) is in the order of the number of iterations multiplied by the number of populations in both GA³⁸ and PSO²⁵ as will be shown next.

Table 3.5

EEM compared with enhanced GA

Design domain & Boundary conditions			
			
(n_x, n_y, V_0)	Coarse mesh (24, 12, 0.5)		Fine mesh (48, 24, 0.5)
Method	EEM	Enhanced GA³⁸	EEM
Strain Energy	66.1	64.4	63.5
Itr.	150	4×10^4	250
Topology			

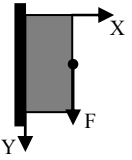




A closer look at the EEM results shows a slight deviation from symmetry. Since EEM is a stochastic method, and domain symmetry is not enforced in the element exchange operation, there is no guarantee to obtain a perfectly symmetric topology even when such a topology is expected at the end. To alleviate this shortcoming that is prevalent in all stochastic techniques, it is possible to model and use only the symmetric portion of the domain, consistent with the loading and support conditions in the problem. Even with the lack of a formal mechanism to enforce symmetry in the final topology, it is interesting to note the appearance of a nearly symmetric topology in EEM results.

Model 3: Model 2 with modified dimensions

In this case, the EEM results in Table 3.6 are compared with those based on PSO as reported by Fourie and Groenwold.²⁵ As in the previous model, the EEM solution converges much faster with no loss of accuracy.

Table 3.6

EEM compared with PSO

Design domain & Boundary conditions				
				
(n_x, n_y, V_0)	Coarse mesh (20, 47, 0.5)		Fine mesh (40, 94, 0.5)	
Method	EEM	PSO ²⁵	EEM	PSO ²⁵
Strain Energy	2.96	Not reported	5.1	Not reported
Itr.	100	10 ⁵	103	10 ³
Topology		 Continuous Density		 Binary Density

It should be noted that in both cases of coarse and fine meshes, SIMP and EEM give similar results. Another point worth noting is the lack of perfect symmetry in both stochastic (EEM and PSO²⁵) results.

Comparing the results in Tables 3.5 and 3.6 also reveals that changing the dimensions of the design domain in a topology optimization problem may completely change the optimum topology.

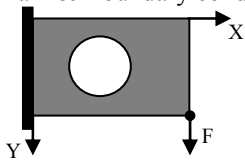




Model 4: Model 1 with a circular hole

The optimal topology for a cantilevered beam with a fixed hole is determined using EEM and the SIMP method. In the case of EEM, the hole is modeled using passive elements. The results shown in Table 3.7 indicate comparable results, with SIMP at $r =$

1.2 converging faster than EEM. It is worth noting that detailed features that are captured by EEM with a coarse mesh only appear in the SIMP results following a mesh refinement.

Table 3.7

Optimal topologies for a cantilever beam with a circular hole

Design domain & Boundary conditions				
				
(n_x, n_y, V_0)	Coarse mesh (60, 40, 0.5)		Fine mesh (90, 60, 0.4)	
Method	EEM	SIMP	EEM	SIMP
Strain Energy	50.48	52.1	51.2	51.9
Itr.	97	34	171	34
Topology				

Comparing the results of Table 3.7 with Table 3.4, one may conclude that the presence of passive elements (regions), other than the problem's dimensions, may also drastically change the optimum topology.

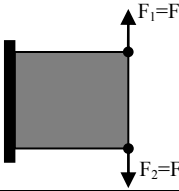




Model 5: Opposing loads at the tip

The optimal topologies for the cantilevered beam model under a bidirectional loading condition are given in Table 3.8. The results reveal some interesting features. The medium-density middle brace in the SIMP result is replaced by two closely spaced members in EEM with nearly the same strain energy values.

Refining the mesh clarifies the image as shown in Table 3.8. Whereas in the SIMP method it is necessary to adjust the filtering size to obtain the best topology, in EEM the solution procedure reveals the most detailed topology that is possible for a given mesh density.

Table 3.8

Optimal topologies for a doubly loaded cantilever beam

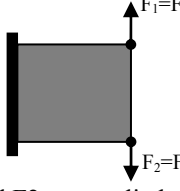


Design domain & Boundary conditions				
				
(n_x, n_y, V_0)	Coarse mesh (32, 20, 0.4)		Fine mesh (50, 50, 0.4)	
Method	EEM	SIMP	EEM	SIMP
Strain Energy	17.48	17.63	19.6	19.7
Itr.	73	37	199	37
Topology				

As seen in Table 3.8, EEM does not yield a perfectly symmetric topology. But looking at the strain energies of the EEM and SIMP results, the slight deviation from symmetry does not alter the strain energy by any significant amount.

If the beam is required to support loads F_1 and F_2 separately (one at a time), then the optimal topology will have a different configuration as shown in Table 3.9.

Table 3.9

Optimum topologies for a doubly loaded cantilever beam

Design domain & Boundary conditions  (F1 and F2 are applied separately)		
$(n_x, n_y, V_0) = (50, 50, 0.4)$		
<i>Method</i>	<i>EEM</i>	<i>SIMP</i>
<i>Strain Energy</i>	60.9	61.3
<i>Itr.</i>	104	60
<i>Topology</i>		

The disappearance of the vertical member on the right side of the EEM-based topology reveals that it does not play an important role in the strain energy of the loaded structure. Instead, the two diagonal members to the right have more material. It may be inferred as an observation of non-uniqueness of the solution in a topology optimization problem.

Three-dimensional cases

In order to evaluate the performance of EEM in topology optimization of three-dimensional structures, some benchmark problems are solved in this chapter. Each three-dimensional design domain is defined according to n_x , n_y , n_z , V_0 values representing the number of finite elements in the x , y , and z directions and the limit on volume fraction,

respectively. As in the previous section, the EEM results are compared with those reported in the literature.

A. Cubic Domain

A cubic domain is simply supported at its four bottom corners and is loaded by four concentrated vertical forces acting at the top surface as shown in Figure 3.3(a). Using the EEM procedure with $(n_x, n_y, n_z, V_0) = (20, 20, 20, 0.08)$, the optimum topology in Figure 3.3(b) is obtained after 178 iterations with a strain energy of 24.1. For comparison, the results obtained by Olhoff et al.⁴⁰ using the optimum microstructure (OM) method is shown in Figure 3.3(c). The gray regions in the Figure 3.3(c) imply intermediate density since the OM method is gradient-based. Also, as in the SIMP method, elements with density less than a threshold value are filtered out in the OM method to arrive at the final topology. Therefore, the final topology may not match the pre-specified volume fraction.

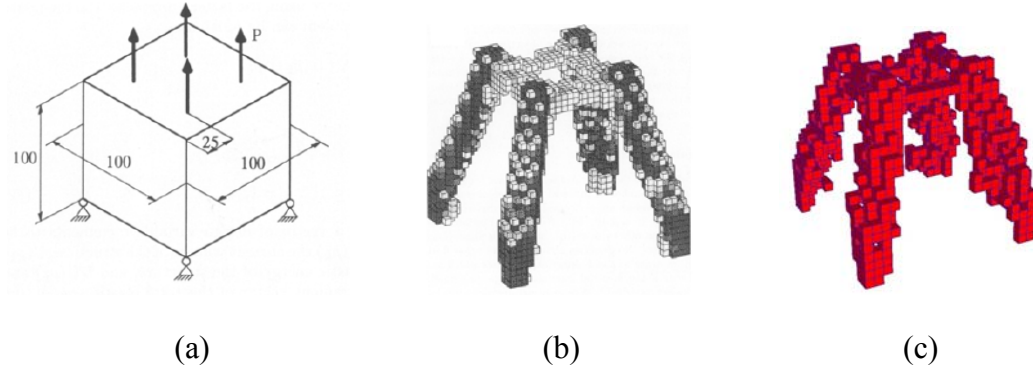


Figure 3.3 EEM compared with optimum microstructure method⁴⁰ in three-dimensional problems; a) Design domain and boundary conditions, b) Optimum microstructures and c) EEM

As seen in the results, the four horizontal bars linking the four columns at the top appear grey in OM result, whereas in EEM they are solid but with less material instead.

B. Cantilevered Beam

A tip-loaded cantilevered beam of finite thickness, as shown in Figure 3.4(a), is optimized for minimum compliance. The EEM results for $(n_x, n_y, n_z, V_0) = (25, 17, 6, 0.3)$ and $(n_x, n_y, n_z, V_0) = (25, 17, 6, 0.1)$ are shown in Figure 3.4(b,c). The EEM solutions for $V_0 = 0.3$ and $V_0 = 0.1$ converge in 206 and 202 iterations, respectively. The OM based solutions reported by Olhoff et al.⁴⁰ for $V_0 = 0.3$ is also shown in Figure 3.4(d). Since the elements with non-dimensional density less than 0.8 are removed in the OM solution, the actual volume fraction is less than that specified. By reducing the volume fraction in EEM, a truss like structure similar to that obtained using the OM method begins to emerge.

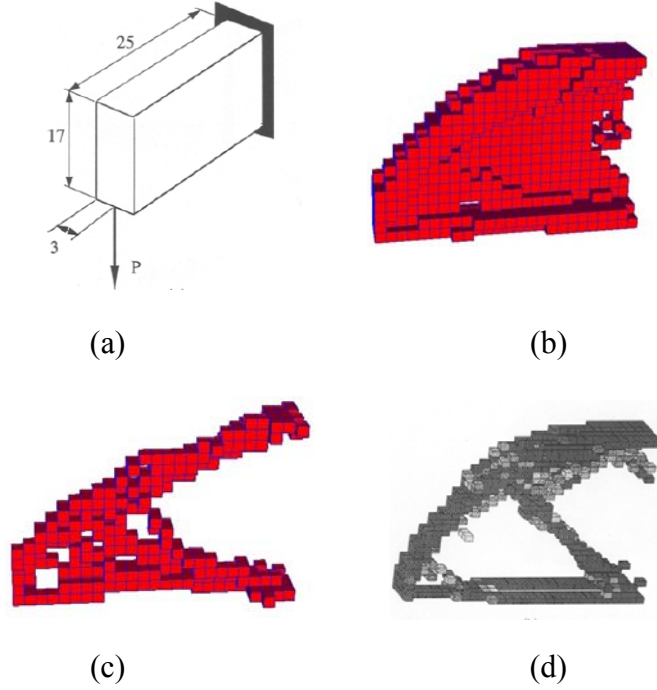


Figure 3.4 EEM compared with optimum microstructure method⁴⁰ in three-dimensional problems; a) Design domain and boundary conditions, b) EEM , $V_f = 0.3$, c) EEM , $V_f = 0.15$ and d) optimum microstructure, $V_f = 0.3$ where elements with the densities less than 0.8 are filtered out

C. Clamped-Clamped Beam

A clamped-clamped beam is loaded in the middle by a concentrated bending moment as shown in Figure 3.5(a). The EEM results for $(n_x, n_y, n_z, V_0) = (50, 10, 10, 0.3)$ and $(n_x, n_y, n_z, V_0) = (50, 10, 10, 0.08)$ are shown in Figure 3.5(b, c). For the OM based solution shown in Figure 3.5(d), the elements with density less than 0.5 are removed. For the same reason stated earlier, the actual volume fraction is less than the specified value of 0.3. Figure 3.5(c) shows that EEM result is sensitive to the direction of the applied moment. It is not clear if a similar sensitivity also exists in the OM based solutions at a

lower volume fraction values. For the solutions in Figure 3.5(b,c), the number of iterations is found to be 197 and 206, respectively.

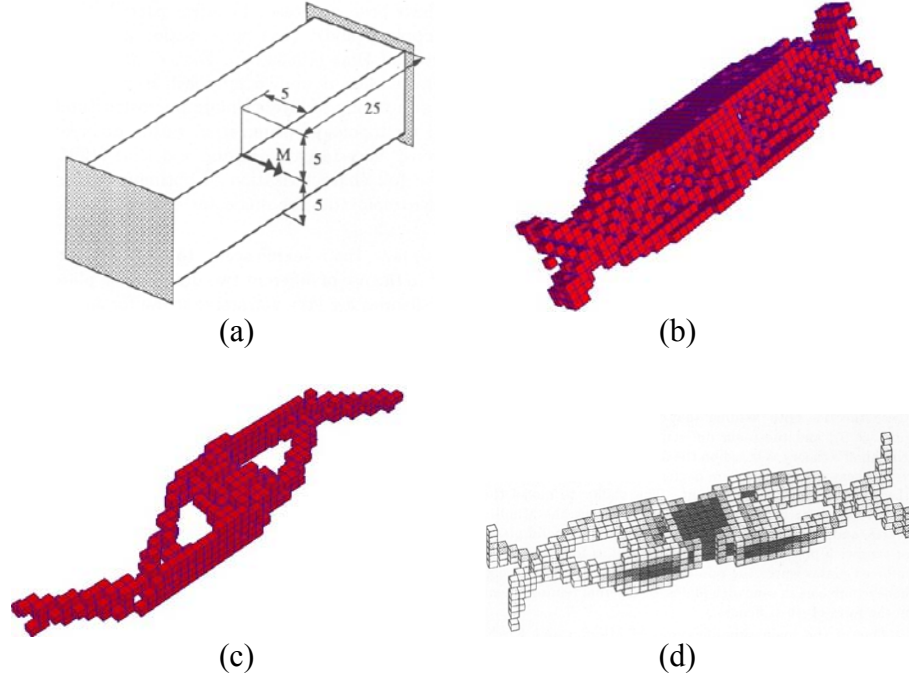


Figure 3.5 EEM compared with optimum microstructure method⁴⁰ in three-dimensional problems; a) Design domain and boundary conditions, b) EEM , $V_f = 0.3$, c) EEM , $V_f = 0.15$ and d) optimum microstructure, $V_f = 0.3$ where elements with the densities less than 0.5 are filtered out

D. Automobile Control Arm

The geometry shown in Figure 3.6(a) is a generic model of an automobile control arm as described in Ref. [41]. While the triangular region in the middle can be altered through topology optimization, the three corner regions (knuckles) are held fixed with the specified boundary conditions. The EEM solution based on $(n_x, n_y, n_z, V_0) = (26, 40, 12, 0.1)$ is shown in Figure 3.6(b) with a final strain energy of 4.5764e4. Since the design domain is symmetric, only the upper half of the final topology is considered and shown

for clarity. The optimization result in Figure 3.6(c) is obtained using a commercial software tool as reported in Ref. [41]. In Figure 3.6(c), the elements with density less than 0.15 are removed and the resulting geometry is post-processed to obtain a smoother shape.

The topology optimization domain for the EEM problem is shown in Figure 3.7. Unlike the model in Ref. [41], the design domain in EEM is modeled as a simple rectangular box surrounded by three smaller regions of passive elements. Based on a random distribution of solid elements, the EEM solution is found following 228 iterations.

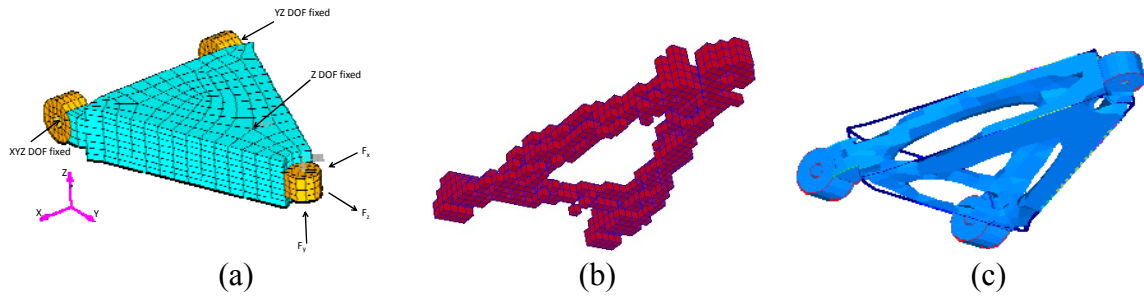


Figure 3.6 Topology optimization of a control arm; a) FE model⁴¹, b) using EEM and c) using OptiStruct⁴¹ software

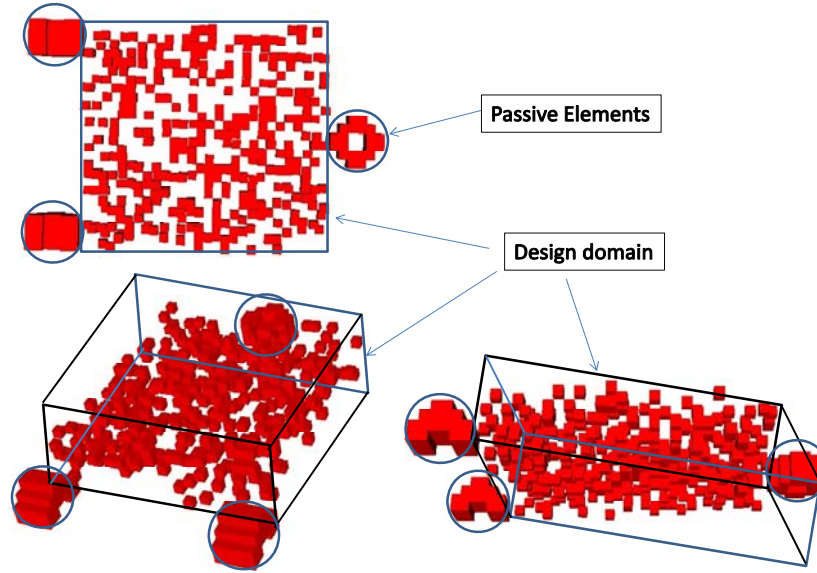


Figure 3.7 Starting point (random distribution of the solid elements) for the control arm problem in EEM

Topology optimization with damaged elements

In some manufacturing processes (e.g., sand casting), it is possible for some regions of the product to be porous, defective or otherwise damaged in terms of material properties. In order to consider the presence of such regions and explore their influence on the optimal topology, several variations to the original topology optimization problem with homogeneous and isotropic material have been considered. Here, a damaged element is defined as one with elastic modulus equal to a fraction of that of a perfect element (e.g., $E_d = 0.1E$ or $E_d = fE$ where f is a random number between 0.01 and 0.9). It should be noted that the damaged elements are treated similar to the passive elements with no participation in the element exchange process.

Figure 3.8 shows the results for the case of the tip-loaded cantilevered beam discussed previously in Table 3.5. In the first case, the topology optimization problem is

solved without any damaged elements with the final topology as shown in Figure 3.8(a). If there is some control over the placing of damaged elements, then their optimum locations will be those shown as grey elements in Figure 3.8(b). In this case, the optimum locations for damaged elements are the locations of solid elements with the lowest level of strain energy, which result in a minimum loss of stiffness. If a specified number of damaged elements are randomly distributed in the optimum topology, then Figure 3.8(c) would be the outcome. The strain energy and the volume fraction of solid (undamaged) elements are shown below each model in Figure 3.8. It is important to note that in Figures 3.8(b) and (c), the damaged elements simply replace the existing solid elements in the optimum topology shown in Figure 3.8(a). Hence, their influence was not captured during the topology optimization process.

Two cases have been studied to optimize the topology with the presence of randomly distributed damaged elements. In the first case, the reduction of the total volume fraction due to the presence of damaged elements has not been compensated with the additional solid elements, whereas in the second case, the total volume fraction is kept constant by adding the equivalent number of solid elements. The outcome for the first case is shown in Figure 3.8(d). Comparing the topology and the strain energy of this case with Figure 3.8(a), one may conclude that the random distribution of damaged elements would not affect the final topology but increases the strain energy of the structure. This seems to be the natural outcome of the reduced stiffness of the structure. However, the reduced stiffness can be compensated with additional solid elements to keep the total volume fraction constant. This will slightly change the material distribution as shown in Figure 3.8(e), but significantly reduces the strain energy.

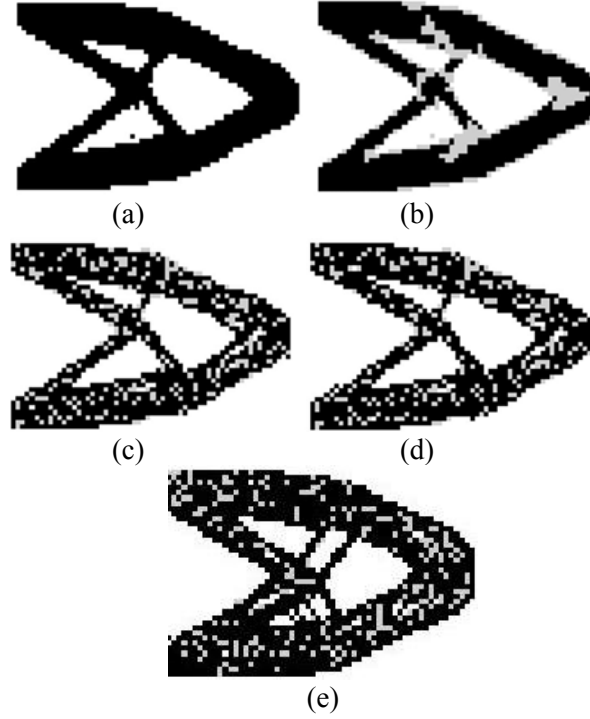


Figure 3.8. a) Optimum topology with no damaged elements ($\mathcal{E}_T = 32.6$), b) optimum arrangement of damaged elements, c) random distribution of damaged elements, d) Optimum topology with an initial random distribution of damaged elements ($\mathcal{E}_T = 42.7$) and e) Optimum topology with an initial random distribution of damaged elements and compensated volume fraction ($\mathcal{E}_T = 35.7$), (in cases (a-d); $V_f = 0.5$, $V_{f_damaged} = 0.2$, $f = 0.2$, in case (e); $V_f = 0.6$)

As a result, one may conclude that the presence of randomly distributed damaged elements may have a local effect on the material distribution but the overall topology remains unaffected.

Strain energy analysis of the elements

As mentioned earlier, the main challenge in EEM is the required number of function calls (FEA plus additional procedures such as filtering). Although this number is

considerably less than those reported for enhanced GA³⁸ and PSO²⁵, it tends to be higher than that in the SIMP method. In each iteration of the EEM algorithm, the element exchange operation takes only 5% of the CPU time with the remaining time spent on solving the FE problem. In pursuit of an approach to make EEM more computationally efficient, we are faced with the following question:

Is it possible to predict the variation in strain energy of the structure by just focusing on the elements that are being exchanged from one iteration to the next and those in their neighborhoods instead of performing an FEA of the whole structure?

To answer this question, the effect of an element exchange on a far-field as well as a neighborhood element has been investigated. Table 3.10 gives the strain energies of the target element at coordinates $(X,Y)_t$ as well as that of the whole structure before and after a solid element at $(X,Y)_s$ is exchanged with a void element at $(X,Y)_v$. The domain topologies before and after each element exchange are shown in Table 3.11 with the exchanged elements highlighted by square boxes.

Table 3.10

Energy variation in a target and the whole domain due to solid-void exchange of an arbitrary element

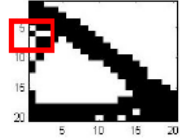
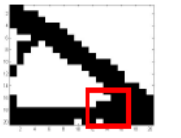
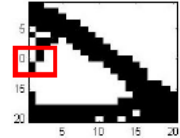
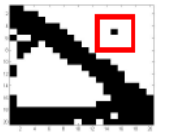
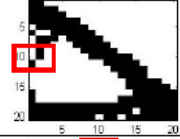
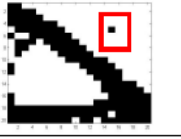
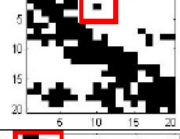
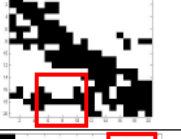
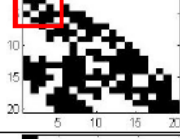
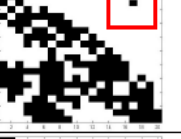
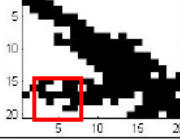
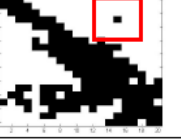
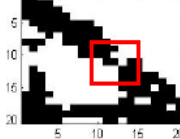
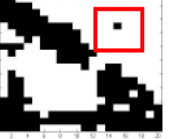
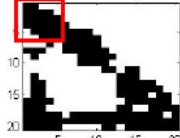

Case #	Iteration #	$(X,Y)_t$	$(X,Y)_s$	$(X,Y)_v$	E_t before	E_t after	E_{whole} before	E_{whole} after
1	149	(2,2)	(1,6)	(15,19)	5.19E-01	6.25E-01	3.17E+01	3.23E+01
2	149	(2,2)	(2,10)	(15,5)	5.19E-01	5.56E-01	3.17E+01	3.20E+01
3	149	(4,7)	(2,10)	(15,5)	3.95E-02	1.90E-02	3.17E+01	3.20E+01
4	21	(2,16)	(10,3)	(8,18)	4.86E-04	1.06E-01	3.79E+02	1.01E+02
5	50	(2,2)	(2,3)	(17,3)	4.84E-01	8.14E-01	1.05E+02	1.05E+02
6	6	(2,2)	(5,17)	(15,5)	5.99E-01	1.41E+01	7.34E+01	1.31E+03
7	120	(2,2)	(12,11)	(15,5)	4.81E-01	9.91E-01	4.28E+01	3.34E+03
8	120	(2,2)	(2,3)	(13,11)	4.81E-01	7.24E-01	4.28E+01	4.25E+01

The topology optimization problem selected for this investigation is that of a cantilevered beam (Table 3.4) with $(n_h, n_v, V_0) = (20, 20, 0.4)$. In Table 3.11, eight different cases are examined with the corresponding iteration numbers at which the exchange is made also identified.

The results indicate that the strain energy of the structure as well as that of each element is mainly affected by the integrity of the structure. In other words, if a critical solid element is removed from the load path, the total strain energy of the structure increases tremendously (Cases 6 and 7). Conversely, if an element connects two disconnected parts of the structure to construct a necessary load path, it will greatly decrease the total energy of the structure (Case 4). In all cases in Table 3.11, the change in strain energy does not depend on how close or how far the exchanged elements are to the target element. Hence, it appears that it is *not* possible to predict the variation in the strain energy of the structure by just focusing on the vicinity of the elements being exchanged, and we have to analyze the whole structure in each iteration.

Table 3.11

Topologies corresponding to each element exchange

Case #	Before Exchange	After Exchange
1		
2		
3		
4		
5		
6		
7		
8		

Strain energy convergence

Figure 3.9 shows how the strain energy in EEM converges to its minimum value for the doubly loaded cantilevered beam case (see Table 3.8). It starts from extremely

large value because of the randomly distributed elements in the initial step. However, after a few iterations, the strain energy reduces to nearly the same order as its minimum value. At this stage, a reasonable load path between the loading points and supports has been constructed, but the topology of the structure is not refined yet. The continuation of the element exchange will refine the topology toward nearly its minimum strain energy. Although there might be some jumps to some higher level during EEM, the overall trend of the strain energy is descendent. The large spikes in the energy convergence plot in Figure 3.9 are mostly attributed to the random shuffle operations in the EEM procedure.

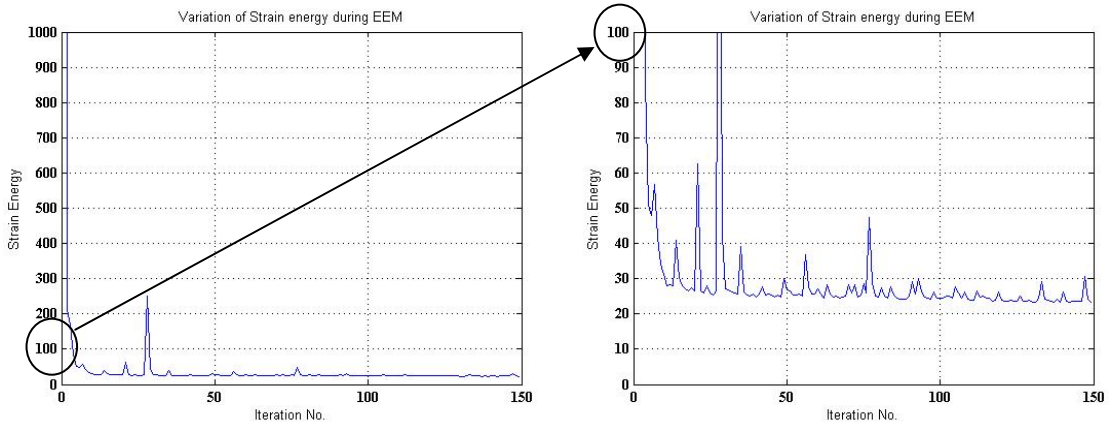


Figure 3.9 Energy convergence in EEM; rapid convergence from high energy (left) and slow convergence in low energy (right)

Effect of EEM parameters on the solution

The EEM parameters including the maximum number of iterations N_s , number of elements to be exchanged N_{EE} , the step sizes for checkerboard L_c , random exchange L_R , and iteration number to start the checkerboard control (i_c) have to be initially specified. All other parameters are calculated from these parameters and the problem inputs

(number of elements, volume fractions, etc.). The higher the value of N_s and the more rigorous the convergence parameters (ε 's) are, the lower the final value of strain energy, but certainly at the expense of higher computational time. Based on our experience, choosing $N_{\max} \sim 5\text{-}10\%$ and $N_{\min} \sim 0.2\text{-}0.4\%$ of the solid elements would be appropriate. Starting from larger N_{\max} value would be similar to a larger coefficient for the particle's velocity in PSO²⁵ and increases the craziness of the search at the beginning steps. This will make finding the global optimum more probable but less computationally efficient. On the other hand, small N_{\min} value makes the solution easier to converge at the very end and provides a more definite final topology. However, for the convergence criteria to make more sense, we should put smaller ε 's that will consequently increase the number of iterations. The step size for random distribution is better set higher in the problems with large number of solid elements or large N_s because in these situations, EEM is less likely to get trapped in a loop (see Element Exchange Strategy part of the EEM algorithm). The checkerboard control, however, should be called in about every 5% of maximum iterations. The values selected for all of these parameters can be adjusted and reasonable deviations from the suggested values may not dramatically affect the final results.

Limitations of EEM

As with many other methods, EEM has its own limitations; some of them can be eliminated in future improvements of the method while others may not. In its present implementation, using quadrilateral elements is a necessity for the checkerboard elimination part of EEM unless another definition of checkerboard is introduced.

As in the case of GA, EEM will not work for very low volume fractions because of the connectivity problem. If the volume fraction is so low and the selected element size is so large that they may not connect the loaded points to the supports, then exchanging the elements may not lead to an optimum topology. Because the topologies obtained from the exchanging procedure are not close enough to the solution domain. This problem is easy to fix though; EEM can start from a large enough volume fraction, and after finding a solution, the design domain can be replaced by the regions which have been occupied with the solid elements of the previous solution. Now, the new problem with a new (large enough) volume fraction in the new design domain will be solved. These procedures continue until we come up with a solution having the desired total low volume fraction (which is the multiplication of all the volume fractions applied in each step).

EEM is not an optimization method in a *mathematical programming* sense. In addition, it is a stochastic technique. These two features, together with the flatness and noisiness of the topology optimization problem cannot guarantee that EEM-based solution is an exact optimum. It also may yield multiple solutions for a single problem when the solutions have very close strain energies as shown in the results.

Since EEM is based on the effectiveness of the individual finite elements, any other objective function or constraint to be considered in the topology optimization problem should be defined so that it is distributable among the elements. In other words each element should have a quantity to be compared with other elements representing its influence on the objective function or design constraint.

CHAPTER IV

CONCLUSIONS AND FUTURE WORK

A new stochastic direct search topology optimization method has been developed and used for compliance minimization problems subject to a volume fraction constraint. The non-dimensional density of each finite element is treated as a binary design variable with a linear element density-stiffness relationship. The basic principle behind the proposed method is that by exchanging the low-strain-energy solid elements with the high-strain-energy void elements from one iteration to the next, an optimum topology will emerge. The Element Exchange Method (EEM) provides converged solutions resulting in minimum strain energy. However, depending on the selected mesh density and the desired level of clarity in the final topology, the number of iterations required for convergence may vary. Through the solution of several two- and three-dimensional example problems, the accuracy and efficiency of EEM were examined and compared with different gradient and non-gradient methods reported in the literature. The presence of damaged elements in the resulted topology has also been studied. It has been shown that randomly distributed damaged elements change the local distribution of material without significantly altering the topology of the optimum structure.

In general, the EEM method is easy to implement and can be directly coupled with any FE code. Unlike the gradient-based methods, it requires no filtering and the

resulting solid-void solution satisfies the imposed volume fraction. The checkerboard control and the random shuffle algorithms help increase the solution fidelity and accuracy. Although EEM is not as efficient as the SIMP method, it is found to be significantly more efficient than many other non-gradient methods reported in the literature such as GA and PSO.

One potential topic for future work is to investigate the inclusion of stress, displacement, or frequency constraints on the EEM procedure. Besides compliance minimization, the maximization of the fundamental frequency could also be considered in an EEM-based optimization problem. In considering other objective functions and design constraints, it is important to properly model the contribution of each element to the selected response function.

Improving the computational efficiency of EEM is another important area for future work. Linking the EEM procedure to a finite element code and using some more efficient computational methods such as parallel algorithms may enable the application of EEM to more complex engineering problems with a very large number of elements and geometric requirements.

REFERENCES

- [1] Sigmund, O., “Topology optimization: a tool for the tailoring of structures and materials”. *A special issue of the Philosophical Transactions of the Royal Society: Science into the next Millennium (Issue III, Mathematics, Physics and Engineering)*, 358(1765):211–227, 2000.
- [2] Bendsøe, M. P., and Kikuchi, N., “Generating Optimal Topologies in Structural Design using a Homogenization Method,” *Computer Methods in Applied Mechanics and Engineering*, Vol. 71, No. 2, 1988, pp.197-224.
- [3] Rozvany, G. I. N., Zhou, M., and Birker, T, “Generalized Shape Optimization Without Homogenization”, *Structural Optimization*, Vol. 6, 1992, pp. 200-204.
- [4] Bendsøe, M. P., and Sigmund, O., *Topology Optimization, theory, methods and applications*, Springer , 2003.
- [5] Sigmund, O., “On the Design of Compliant Mechanisms using Topology Optimization”, *Mechanics of Structures and Machines*, Vol. 25, No. 4, 1997, pp. 493-524.
- [6] Sigmund, O., “Optimum Design of Microelectromechanical Systems”, *Mechanics for a New Millennium, Proceedings of the 20th International Congress of Theoretical and Applied Mechanics Chicago, Illinois, USA, 27 August – 2 September 2000*, pp. 505-520.
- [7] Sigmund, O., “Design of Multiphysics Actuators using Topology Optimization-Part I: One-material Structures”, *Computer Methods in Applied Mechanics and Engineering*, Vol. 190, Issues 49-50, 2001, pp. 6577-6604.
- [8] Bendsøe, M. P., Lund, E., Olhoff, N., and Sigmund, O., “*Topology optimization – broadening the areas of application*”, *Control and Cybernetics*, vol. 34 (2005) No. 1, pp 7-35.
- [9] Sigmund, O., “Design of material structures using topology optimization”, DCAMM Report S.69 , department of solid mechanics, Ph.D. Thesis, DTU, 1994.

- [10] Sigmund, O., and Petersson, J., "Numerical Instabilities in Topology Optimization: A Survey on Procedures Dealing with Checkerboards, Mesh-Dependencies and Local Minima," *Structural Optimization*, Vol. 16, No. 1, 1998, pp. 68-75.
- [11] Bendsøe, M. P., "Optimal Shape Design as a Material Distribution Problem," *Journal of Structural and Multidisciplinary Optimization*, Vol. 1, No. 4, 1989, pp. 193-202.
- [12] Zhou, M., and Rozvany, G. I. N., "The COC algorithm, part II: Topological, Geometry and Generalized Shape Optimization," *Computer Methods in Applied Mechanics and Engineering*, Vol. 89, No. 1-3, 1991, pp. 197-224.
- [13] Eschenauer, H. A., and Olhoff, N., "Topology Optimization of Continuum Structures: A Review". *Appl. Mech. Rev.*, 54(4):331–390, July 2001.
- [14] Wang, S., "Krylov Subspace Methods for Topology Optimization on Adaptive Meshes", PhD Dissertations, University of Illinois at Urbana-Champaign, 2007.
- [15] Svanberg, K., "Method of Moving Asymptotes - a New Method for Structural Optimization", *Int. J. Num. Meth. Eng.*, vol 24, pp. 359-373, 1987.
- [16] Rozvany, G. I. N., "A Critical Review of Established Methods of Structural Topology Optimization," *Structural and Multidisciplinary Optimization*, Vol. 37, No. 3, 2009, pp. 217-237.
- [17] Sigmund, O., "A 99 Line Topology Optimization Code Written in Matlab," *Structural and Multidisciplinary Optimization*, Vol. 21, No. 2, 2001, pp. 120-127.
- [18] Diaz, A. R., and Sigmund, O., "Checkerboard Patterns in Layout Optimization", *Structural Optimization*, 10, 1995, pp. 40-45.
- [19] Jog, C. S., and Haber, R. B., "Stability of Finite Element Models for Distributed Parameter Optimization and Topology Design," *Computer Methods in Applied Mechanics and Engineering*, Vol. 130, No. 3, 1996, pp. 203-226.
- [20] Haber, R. B., Jog, C. S., and Bendsoe, M. P., "A New Approach to Variable-Topology Design Using a Constraint on the Perimeter," *Structural Optimization*, Vol. 11, No. 1-2, 1996, pp. 11-12.
- [21] Guo, X., and Gu, Y. X., "A New Density-Stiffness Interpolation Scheme for Topology Optimization of Continuum Structures," *Engineering Computations*, Vol. 21, No. 1, 2004, pp. 9-22.

- [22] Bruns, T. E., "A Reevaluation of the SIMP Method with Filtering and an Alternative Formulation for Solid-Void Topology Optimization," *Structural and Multidisciplinary Optimization*, Vol. 30, No. 6, 2005, pp. 428-436.
- [23] Fuchs, M. B, Jiny, S., and Peleg, N. "The SRV Constraint for 0/1 Topological Design," *Structural and Multidisciplinary Optimization*, Vol. 30, No. 4, 2005, pp. 320-326.
- [24] Mattheck, C., and Burkhardt, S., "A New Method of Structural Shape Optimization Based on Biological Growth," *International Journal of Fatigue*, Vol. 12, No. 3, 1990, pp. 185-190.
- [25] Fourie, P. C., and Groenwold, A. A., "The Particle Swarm Algorithm in Topology Optimization," In Proceedings of the Fourth World Congress of Structural and Multidisciplinary Optimization, Dalian, China., 2001.
- [26] Xie, Y. M., and Steven, G. P., "A Simple Evolutionary Procedure for Structural Optimization," *Engineering Computations*, Vol. 49, No. 5, 1993, pp. 885-896.
- [27] Querin, O. M., Steven, G. P., and Xie, Y. M., "Evolutionary Structural Optimization (ESO) Using a Bidirectional Algorithm," *Computer and Structures*, Vol. 15, No. 8, 1998, pp. 1031-1048.
- [28] Liu, J. S., Parks, G. T., and Clarkson, P. J., "Metamorphic Development: A New Topology Optimization Method for Continuum Structures," *Structural and Multidisciplinary Optimization*, Vol. 20, No. 4, 2000, pp. 288-300.
- [29] Goldberg, D. E., Genetic Algorithms in Search, Optimization, and Machine Learning, New York: Addison-Wesley, 1989.
- [30] Kita, E. and Toyoda, T., "Structural Optimization Using Local Rules," In Proceedings of Third World Congress of Structural and Multidisciplinary Optimization, Niagara Falls, N.Y., USA, May 1999. Paper no. 30-SMD-3.
- [31] Kutyłowski, R., "On Nonuniqueness Solutions in Topology Optimization," *Structural and Multidisciplinary Optimization*, Vol. 23, No. 5, 2002, pp. 398-403.
- [32] Werner, M., "Globally Optimal Benchmark Solutions to Some Small-Scale Discretized Continuum Topology Optimization Problems," *Structural and Multidisciplinary Optimization*, Vol. 32, No. 3, 2006, pp. 259-262.
- [33] Mei, Y., L., Wang, X. M., and Cheng, G. D., "Binary Discrete Method of Topology Optimization," *Applied Mathematics and Mechanics*, Vol. 28, No. 6, 2007, pp. 707-719.

- [34] <http://www.topopt.dtu.dk/Theory1/afs5.html>.
- [35] Rouhi, M., and Rais-Rohani, M., "Topology Optimization of Continuum Structures Using Element Exchange Method," 49th AIAA/ASME/ASCE/AHS/ASC Structures, Structural Dynamics, and Materials, 7 - 10 April 2008, Schaumburg, IL.
- [36] Olhoff, N.; Bendsoe, M.P., and Rasmussen, J., "On CAD integrated structural topology and design optimization," *Comput Methods Appl Mech Eng* 89, 1991, 259–279.
- [37] Wang, M. Y., and Wang, X., "Level Set Models for Structural Topology Optimization," Proceedings of DETC'03, ASME 2003 Design Engineering Technical Conferences and ASME 2003 Design Engineering Technical Conferences and Computers and Information in Engineering Conference, Chicago, IL, 2-6 Sep. 2003.
- [38] Wang, S. Y., Tai, K., and Wang, M. Y., "An Enhanced Genetic Algorithm for Structural Topology Optimization," *Int. J. Numer. Meth. Engng.*, Vol. 65, No. 1, 2006, pp. 18-44.
- [39] Jakiela, M. J., Chapman, C., Duda, J., Adewuya, A., and Saitou, K., "Continuum Structural Topology Design with Genetic Algorithms," *Comput. Methods Appl. Mech. Engrg.*, Vol. 186, No. 2-4, 2000, pp. 339-356.
- [40] Olhoff, N., Ronholt, E., and Scheel, J., "Topology Optimization of three-dimensional structures using optimum microstructures," *Structural Optimization*, Vol. 16, No. 1, 1998, pp. 1-18.
- [41] <http://www.kxcad.net/Altair/HyperWorks/ostutorials/ostut.htm#os2010.htm>.

APPENDIX

MATLAB^{7.0} CODE* FOR A CANTILEVERED BEAM WITH A CIRCULAR HOLE

(SEE TABLE 3.7)

The author acknowledged the FEA part of the code provided by Sigmund.¹⁷

```
function topen(nelx,nely,volfrac);
volfrac = 0.45;
nelx = 70;
nely = 45;
xmin = 0.001;
vol = nelx*nely*xmin;
x(1:nely,1:nelx) = xmin;
xbest(1:nely,1:nelx) = 0;
enbest(1:nely,1:nelx) = 0;
delta_x = 1000;
delta_e = 1000;
enormalized = 100;
cold = 0.;
cbest = 1e10;
c = 0.;
cnew = 1;
loopmax = 150;
randstep = 7;
chbstep = 4;
stchb = 20;%start checkerboard
nreemax = 50;
nreemin = 5;
nree = nreemax;
neemax = 50;
neemin = 5;
neegdstep = 7;
nee = neemax;

%%%%%%%%%%%%%%%%%%%%%%%%%%%%%%%%%%%%%%%%%%%%%%%%%%%%%%%%%%%%%%%%%%%%%%%%
% (Start) Defining the design domain%%%%%%%%%%%%%%%%%%%%%%%%%%%%%%%%%%%%%%%%%%%%%%%%%%%%%%%%%%%%%%%%%%%%%%%%
%%%%%%%%%%%%%%%%%%%%%%%%%%%%%%%%%%%%%%%%%%%%%%%%%%%%%%%%%%%%%%%%%%%%%%%%
for ely = 1: nely
    for elx = 1:nelx
        if (sqrt((ely-nely/2.)^2+(elx-nelx/3.)^2) < nely/3)
            passive(ely,elx) = 1;
            x(ely,elx) = xmin;
        else
            passive(ely,elx) = 0;
        end
    end
end
%%%%%%%%%%%%%%%%%%%%%%%%%%%%%%%%%%%%%%%%%%%%%%%%%%%%%%%%%%%%%%%%%%%%%%%%
```

%%(End)Defining the design domain %%%%%%%%%%%
 %%%%%%%%%%

%%%%%%%%%
 (Start) Random distribution of the elements in the design domain with specified volume
 fraction %%%%%%%%%%
 %%%%%%%%%%

```
while vol < volfrac*nelx*nely
    l = 1 + round(rand*(nely-1));
    k = 1 + round(rand*(nelx-1));
    if ((x(l,k) < 0.5) & (passive(l,k) == 0));
        x(l,k) = 1;
        vol = vol + x(l,k);
    end
end
```

```
xbest = x;
%%%%%%%%%
```

(End) Random distribution of the elements in the design domain with specified volum
 fraction %%%%%%%%%%
 %%%%%%%%%%

```
gdst = 0;
loop = 0;
gdstpsize = (loopmax/neegdstep);
kd = 0;
tic;
while ((loop < loopmax+100 & (delta_x > 20 | enormalized > 0.001)) | (delta_x == 0) )
    loop = loop + 1
    gdst = floor(loop/gdstpsize)-floor((loop-1)/gdstpsize);
    if gdst > 0
        kd = kd+1;
        nee = max (floor(neemax - kd*(neemax-neemin)/(neegdstep)),neemin)
        nree = max(floor(nreemax - kd*(nreemax-nreemin)/(neegdstep)),nreemin)
    end
```

%%%%%%%%%
 %(Start) After "randstep" iterations "nree" elements will be exchanged from "xmin" to
 "1" and vice versa%%%%%%%%%
 crzns = fix(floor((loop)/randstep)/(loop)/randstep));

```
if crzns > 0.5
    for m = 1:nree
        randy = 1 + round(rand*(nely-1));
        randx = 1 + round(rand*(nelx-1));
        while (x(randy,randx) > 0.5 | passive(randy,randx) == 1)
```



```

        rdy = 1 + round(rand*(nely-1));
        rdx = 1 + round(rand*(nelx-1));
    end
    x(rdy,rdx) = 1;
end

for n = 1:nree
    rdy = 1 + round(rand*(nely-1));
    rdx = 1 + round(rand*(nelx-1));
    while (x(rdy,rdx) < 0.5 | passive(rdy,rdx) == 1)
        rdy = 1 + round(rand*(nely-1));
        rdx = 1 + round(rand*(nelx-1));
    end
    x(rdy,rdx) = xmin;
end
end
%%%%%%%%%%%%%%%%%%%%%%%%%%%%%%%%%%%%%%%%%%%%%%%%%%%%%%%%%%%%%%%%%%%%%%%%%%
%%(End) After "randstep" iterations "nree" elements will be exchanged from "xmin" to
"1" and vice versa %%%%%%%%%%%%%%%%%%%%%%%%%%%%%%%%%%%%%%%%%%%%%%%%%%%%%%%%%%%%%%%%%%%%%%%%%%%
%%%%%%%%%%%%%%%%%%%%%%%%%%%%%%%%%%%%%%%%%%%%%%%%%%%%%%%%%%%%%%%%%%%%%%%%%%

%%%%%%%%%%%%%%%%%%%%%%%%%%%%%%%%%%%%%%%%%%%%%%%%%%%%%%%%%%%%%%%%%%%%%%%%%%
%(Start) After "chbstep" iterations checkerboard elements will be randomly redistributed
in their pair locations %%%%%%%%%%%%%%%%%%%%%%%%%%%%%%%%%%%%%%%%%%%%%%%%%%%%%%%%%%%%%%%%%%%%%%%%%%%
%%%%%%%%%%%%%%%%%%%%%%%%%%%%%%%%%%%%%%%%%%%%%%%%%%%%%%%%%%%%%%%%%%%%%%%%%%
chb = fix(floor((loop)/chbstep)/((loop)/chbstep))*max(1,stchb/loop);
nchb_s = 0;
xychb_s = zeros(nely,nelx);
nchb_v = 0;
xychb_v = zeros(nely,nelx);
if chb > 0.5
    for m = 2:nely-1
        for n = 2:nelx-1
            if ((x(m,n)>0.5) & (x(m,n-1)<0.5) & (x(m,n+1)<0.5) & ...
                (x(m-1,n)<0.5) & (x(m+1,n)<0.5))
                nchb_s = nchb_s + 1;
                xychb_s(m,n) = 1;
            end
            if ((x(m,n)<0.5) & (x(m,n-1)>0.5) & (x(m,n+1)>0.5) & ...
                (x(m-1,n)>0.5) & (x(m+1,n)>0.5))
                xychb_v(m,n) = 1;
            end
        end
    end
end

```

```

end
for i = 2:nely-1
    for j = 2:nelx-1
        if (xychb_s(i,j) == 1)
            x(i,j) = xmin;
        end
        if ((xychb_v(i,j) == 1) & (xychb_s(i+1,j) ~= 1) &...
            (xychb_s(i-1,j) ~= 1) & (xychb_s(i,j+1) ~= 1) &...
            (xychb_s(i,j-1) ~= 1))
            x(i,j) = 1;
            nchb_v = nchb_v + 1;
        end
    end
end
end
if (nchb_s > nchb_v)
    for m = 1:(nchb_s-nchb_v)
        rdy = 1 + round(rand*(nely-1));
        rndx = 1 + round(rand*(nelx-1));
        while (x(rdy,rndx) > 0.5 | passive(rdy,rndx) == 1)
            rdy = 1 + round(rand*(nely-1));
            rndx = 1 + round(rand*(nelx-1));
        end
        x(rdy,rndx) = 1;
    end
end
if (nchb_v > nchb_s)
    for n = 1:(nchb_v-nchb_s)
        rdy = 1 + round(rand*(nely-1));
        rndx = 1 + round(rand*(nelx-1));
        while x(rdy,rndx) < 0.5
            rdy = 1 + round(rand*(nely-1));
            rndx = 1 + round(rand*(nelx-1));
        end
        x(rdy,rndx) = xmin;
    end
end
end

```

%%%%%%%%%%
 %(End) After "chbstep" iterations checkerboard elements will be randomly redistributed
 in their pair locations %%%%%%%%%%
 %%%%%%%%%%

```

% FE-ANALYSIS%%%%%%%%%%%%%%%%%%%%%%%%%%%%%%%%%%%%%%%%%%%%%%%%%%%%%%%%%%
[U]=FE(nelx,nely,x);
% OBJECTIVE FUNCTION AND SENSITIVITY ANALYSIS%%%%%%%%%%%%%%%%%%%%%%%%%%%%%%%%
[KE] = lk;
elymax_v = zeros(1,nee);
elxmax_v = zeros(1,nee);
enmax_v = zeros(1,nee);
elymin_s = zeros(1,nee);
elxmin_s = zeros(1,nee);
enmin_s = 1e10*ones(1,nee);
cold = c;
c = 0.;
en(1:ely,1:elx) = 0;
for ely = 1:nely
    for elx = 1:nelx
        n1 = (nely+1)*(elx-1)+ely;
        n2 = (nely+1)* elx  +ely;
        Ue = U([2*n1-1;2*n1; 2*n2-1;2*n2; 2*n2+1;2*n2+2; 2*n1+1;2*n1+2],1);
        c = c + x(ely,elx)*Ue'*KE*Ue;
        en(ely,elx) = x(ely,elx)*Ue'*KE*Ue;

%%%%%%%%%%%%%%%%%%%%%%%%%%%%%%%%%%%%%%%%%%%%%%%%%%%%%%%%%%
%%%%%%%%%%%%%%%%%%%%%%%%%%%%%%%%%%%%%%%%%%%%%%%%%%%%%%%%%%
%(Start) Sort the energy of the elements and keep "nee" elements to be exchanged with
their pairs%%%%%%%%%%%%%%%%%%%%%%%%%%%%%%%%%%%%%%%%%%%%%%%%%%%%%%%%%%
%%%%%%%%%%%%%%%%%%%%%%%%%%%%%%%%%%%%%%%%%%%%%%%%%%%%%%%%%%
if x(ely,elx) < 0.5
    if (enmax_v(1,nee) < en(ely,elx) & passive(ely,elx) == 0)
        for i = 1:nee-1
            elymax_v(1,i) = elymax_v(1,i+1);
            elxmax_v(1,i) = elxmax_v(1,i+1);
            enmax_v(1,i) = enmax_v(1,i+1);
        end
        elymax_v(1,nee) = ely;
        elxmax_v(1,nee) = elx;
        enmax_v(1,nee) = en(ely,elx);

    else
        for k = 1:nee-1
            if (en(ely,elx) > enmax_v(1,k)) & (en(ely,elx) < enmax_v(1,k+1)...
                & passive(ely,elx) == 0)
                for l = 1:k-1

```

```

        elymax_v(1,l) = elymax_v(1,l+1);
        elxmax_v(1,l) = elxmax_v(1,l+1);
        enmax_v(1,l) = enmax_v(1,l+1);
    end
    elymax_v(1,k) = ely;
    elxmax_v(1,k) = elx;
    enmax_v(1,k) = en(ely,elx);
end

end

end
else
    if (enmin_s(1,nee) > en(ely,elx) & passive(ely,elx) == 0);
        for j = 1:nee-1
            elymin_s(1,j) = elymin_s(1,j+1);
            elxmin_s(1,j) = elxmin_s(1,j+1);
            enmin_s(1,j) = enmin_s(1,j+1);
        end
        elymin_s(1,nee) = ely;
        elxmin_s(1,nee) = elx;
        enmin_s(1,nee) = en(ely,elx);

    else
        for k = 1:nee-1
            if (en(ely,elx) < enmin_s(1,k)) & (en(ely,elx) > enmin_s(1,k+1)...
                & passive(ely,elx) == 0)
                for l = 1:k-1
                    elymin_s(1,l) = elymin_s(1,l+1);
                    elxmin_s(1,l) = elxmin_s(1,l+1);
                    enmin_s(1,l) = enmin_s(1,l+1);
                end
                elymin_s(1,k) = ely;
                elxmin_s(1,k) = elx;
                enmin_s(1,k) = en(ely,elx);
            end
        end

    end
end
end
end

```

%%%%%%%%%%
 %(End) Sort the energy of the elements and keep "nee" elements to be exchanged with
 their pairs%%%%%%%%%

```

%%%%%%%%%%%%%%%%%%%%%%%%%%%%%%%%%%%%%%%%%%%%%%%%%%%%%%%%%%%%%%%%%%%%%%%%
%%%%%%%%%%%%%%%%%%%%%%%%%%%%%%%%%%%%%%%%%%%%%%%%%%%%%%%%%%%%%%%%%%%%%%%%
    end
end
cnew = c
if cnew < cbest
    xbestprev = xbest;
    enprevbest = enbest;
    xbest = x;
    enbest = en;
    cbest = cnew;

    delta_e = 0;
    delta_x = 0;
    for ely = 1:nely
        for elx = 1:nelx
            delta_e = delta_e + (enbest(ely,elx)-enprevbest(ely,elx))^2;
            delta_x = delta_x + (xbest(ely,elx)-xbestprev(ely,elx))^2;
        end
    end
    enormalized = delta_e/cbest;
end
cbest
delta_x
delta_e
enormalized

%%%%%%%%%%%%%%%%%%%%%%%%%%%%%%%%%%%%%%%%%%%%%%%%%%%%%%%%%%%%%%%%%%%%%%%%
%%%%%%%%%%%%%%%%%%%%%%%%%%%%%%%%%%%%%%%%%%%%%%%%%%%%%%%%%%%%%%%%%%%%%%%%
%(Start) "nee" elements exchange%%%%%%%%%%%%%%%%%%%%%%%%%%%%%%%%%%%%%%%%%%%%%%%%%%%%%%%%%%%%%%%%%%%%%%%%
%%%%%%%%%%%%%%%%%%%%%%%%%%%%%%%%%%%%%%%%%%%%%%%%%%%%%%%%%%%%%%%%%%%%%%%%
for m = 1:nee
    x(elymin_s(1,m),elxmin_s(1,m)) = xmin;
    x(elymax_v(1,m),elxmax_v(1,m)) = 1;
end
%%%%%%%%%%%%%%%%%%%%%%%%%%%%%%%%%%%%%%%%%%%%%%%%%%%%%%%%%%%%%%%%%%%%%%%%
%%%%%%%%%%%%%%%%%%%%%%%%%%%%%%%%%%%%%%%%%%%%%%%%%%%%%%%%%%%%%%%%%%%%%%%%
%(End) "nee" elements exchange%%%%%%%%%%%%%%%%%%%%%%%%%%%%%%%%%%%%%%%%%%%%%%%%%%%%%%%%%%%%%%%%%%%%%%%%
%%%%%%%%%%%%%%%%%%%%%%%%%%%%%%%%%%%%%%%%%%%%%%%%%%%%%%%%%%%%%%%%%%%%%%%%
hold on;
subplot(1,2,1)
colormap(gray); imagesc(-x); axis equal; axis tight; axis off; pause(1e-6);
subplot(1,2,2)

```

```

colormap(gray); imagesc(-xbest); axis equal; axis tight; axis off; pause(1e-6);
end
toc;
t = toc
%%%%%%%%%%%%%%%%%%%%%%%%%%%%%%%%%%%%%%%%%%%%%%%%%%%%%%%%%%%%%%%%%%%%%%%%
%FE-ANALYSIS %%%%%%%%%%%%%%
%%%%%%%%%%%%%%%%%%%%%%%%%%%%%%%%%%%%%%%%%%%%%%%%%%%%%%%%%%%%%%%%%%%%%%%%
function [U]=FE(nelx,nely,x)
[KE] = lk;
K = sparse(2*(nelx+1)*(nely+1), 2*(nelx+1)*(nely+1));
F = sparse(2*(nely+1)*(nelx+1),1); U = sparse(2*(nely+1)*(nelx+1),1);
for elx = 1:nelx
    for ely = 1:nely
        n1 = (nely+1)*(elx-1)+ely;
        n2 = (nely+1)* elx  +ely;
        edof = [2*n1-1; 2*n1; 2*n2-1; 2*n2; 2*n2+1; 2*n2+2; 2*n1+1; 2*n1+2];
        K(edof,edof) = K(edof,edof) + x(ely,elx)*KE;
    end
end
% DEFINE LOADS AND SUPPORTS (HALF MBB-BEAM)
F(2*(nelx+1)*(nely+1),1) = -1;
fixeddofs = [1:2*(nely+1)];
alldofs = [1:2*(nely+1)*(nelx+1)];
freedofs = setdiff(alldofs,fixeddofs);
% SOLVING
U(freedofs,:) = K(freedofs,freedofs) \ F(freedofs,:);
U(fixeddofs,:)= 0;
%%%%%%%%%%%%%%%%%%%%%%%%%%%%%%%%%%%%%%%%%%%%%%%%%%%%%%%%%%%%%%%%%%%%%%%%
% ELEMENT STIFFNESS MATRIX %%%%%%%%%%%%%%
%%%%%%%%%%%%%%%%%%%%%%%%%%%%%%%%%%%%%%%%%%%%%%%%%%%%%%%%%%%%%%%%%%%%%%%%
function [KE]=lk
E = 1.;
nu = 0.3;
k=[ 1/2-nu/6  1/8+nu/8 -1/4-nu/12 -1/8+3*nu/8 ...
    -1/4+nu/12 -1/8-nu/8  nu/6      1/8-3*nu/8];
KE = E/(1-nu^2)*[ k(1) k(2) k(3) k(4) k(5) k(6) k(7) k(8)
    k(2) k(1) k(8) k(7) k(6) k(5) k(4) k(3)
    k(3) k(8) k(1) k(6) k(7) k(4) k(5) k(2)
    k(4) k(7) k(6) k(1) k(8) k(3) k(2) k(5)
    k(5) k(6) k(7) k(8) k(1) k(2) k(3) k(4)
    k(6) k(5) k(4) k(3) k(2) k(1) k(8) k(7)
    k(7) k(4) k(5) k(2) k(3) k(8) k(1) k(6)
    k(8) k(3) k(2) k(5) k(4) k(7) k(6) k(1)];

```

69